

*A Project Report on*  
**ANALYSIS OF BURIED PIPELINES IN EARTHQUAKE-PRONE  
REGIONS LIKE ASSAM**

*Submitted in partial fulfillment of the requirements for the award of the degree of*

**MASTER OF TECHNOLOGY**  
in  
**CIVIL ENGINEERING**

*(With specialization in Geotechnical Engineering)*

Under

**ASSAM SCIENCE AND TECHNOLOGY UNIVERSITY**

SESSION: 2022-2024



Submitted by:

**PRIANCI KASHYAP**

**M.TECH 4<sup>th</sup> Semester**

**Roll No: PG/C/22/15**

**ASTU Registration No: 324108118 of 2018-2019**

Under the guidance of:

**DR. ABINASH MAHANTA**  
Assistant Professor

**DR. JAYANTA PATHAK**  
HoD, Professor

**Department of Civil Engineering**

**ASSAM ENGINEERING COLLEGE**

**JALUKBARI, GUWAHATI-13, ASSAM**

## **DECLARATION**

I hereby declare that the work presented in the dissertation “**ANALYSIS OF BURIED PIPELINES IN EARTHQUAKE-PRONE REGIONS LIKE ASSAM**” in partial fulfillment of the requirement for the award of the degree of “**MASTER OF TECHNOLOGY**” in Civil Engineering (With specialization in Geotechnical Engineering), submitted in the Department of Civil Engineering, Assam Engineering College, Jalukbari, Guwahati-13 under Assam Science & Technology University, is a real record of the work carried out in the said college for twelve months under the supervision of Dr. Abinash Mahanta, Assistant Professor and Dr. Jayanta Pathak, HoD, Professor, Department of Civil Engineering , Assam Engineering College, Jalukbari, Guwahati-13.

Do hereby declare that this project report is solemnly done by me and is my effort and that no part of it has been plagiarized without citation.

Date: 15/07/2024

**PRIANCI KASHYAP**

This is to certify that the above statement made by the candidate is correct to the best of my knowledge.

**DR. ABINASH MAHANTA**  
**Assistant Professor**  
**Department of Civil Engineering**  
**Assam Engineering College**

**DR. JAYANTA PATHAK**  
**HoD, Professor**  
**Department of Civil Engineering**  
**Assam Engineering College**

## CERTIFICATE OF SUPERVISION

This is to certify that the work presented in this report entitled — **Analysis of buried pipelines in earthquake-prone regions like Assam** is carried out by Prianci Kashyap, Roll No: PG/C/015, a student of M.Tech 4<sup>th</sup> semester, Department of Civil Engineering, Assam Engineering College, under my guidance and supervision and submitted in the partial fulfillment of the requirement for the award of the Degree of Master of Technology in Civil Engineering with specialization in Geotechnical Engineering under Assam Science and Technology University.

Date: 15/07/2024

Place: Guwahati

DR. ABINASH MAHANTA

Assistant Professor,

Department of Civil Engineering,

Assam Engineering College,

Jalukbari, Guwahati-781013

## **Certificate from the Head of the Department**

This is to certify that the following student of M.Tech 3rd semester of Civil Engineering Department (Geotechnical Engineering), Assam Engineering College, has submitted her project on — **Analysis of buried pipelines in earthquake-prone regions like Assam** in partial fulfillment of the requirement for the award of the Degree of Master of Technology in Civil Engineering with specialization in Geotechnical Engineering under Assam Science and Technology University.

Name: PRIANCI KASHYAP

College Roll No: PG/C/22/15

ASTU Roll No: 220620062014

ASTU Registration No: 324108118 of 2018-2019

Date: 15/07/2024

Place: Guwahati

DR. JAYANTA PATHAK

Professor & Head of the Department

Department of Civil Engineering

Assam Engineering College

Jalukbari, Guwahati- 781013

## ACKNOWLEDGEMENT

I would like to express my sincere appreciation to my supervisor Dr. Abinash Mahanta, Assistant Professor, and Dr. Jayanta Pathak, Professor & HoD, Department of Civil Engineering of Assam Engineering College for his extensive support and encouragement throughout the project work. I am highly indebted for his guidance and constant supervision as well as for providing necessary information regarding the project work. Working under him has indeed been a great experience and inspiration for me.

This project would not have been possible without the help of several individuals who in one way or another contributed and extended their valuable assistance in the preparation and completion of this study.

I express my gratitude towards the entire fraternity of the Department of Civil Engineering of Assam Engineering College.

I cannot help myself without thanking Assam Engineering College, which provided us the required infrastructure and comforts all throughout this course and my project in particular.

Date: 15/07/2024

PRIANCI KASHYAP

Place: Guwahati

M.Tech, 4<sup>th</sup> Semester

Geotechnical Engineering

Department of Civil Engineering

Assam Engineering College

Jalukbari, Guwahati-13

## **ABSTRACT**

---

In earthquake-prone Assam, safeguarding vital infrastructure, especially buried water pipelines, is imperative for effective disaster risk reduction. This report presents a comprehensive study evaluating Guwahati City's pipeline network, assessing its condition, vulnerabilities, and historical performance. The study applies IITK-GSDMA guidelines to design and assess the seismic resilience of buried pipelines. An Excel sheet, developed based on these guidelines, incorporates site-specific data for Guwahati derived from previous earthquake data and literature. Parametric studies analyze strain variations for different pipe diameters and thicknesses under seismic loading conditions. The study also proposes the use of geophysical methods such as Electrical Resistivity Tomography (ERT) and Ground Penetrating Radar (GPR) for monitoring the functioning of pipelines post-installation and following seismic events.

## LIST OF TABLES

Table Number	Description	Page Number
3.6.1	Importance factor for different Classes of Pipeline (Ip)	18
3.6.2	Peak Ground Acceleration as per Seismic Zones	18
3.7.1	Ramberg-Osgood parameters for steel pipe	19
3.8.1	Allowable strain criteria for continuous pipeline	20
4.1	Ground strain induced by seismic waves (along a pipeline)	28
4.2	Some commonly-used pipeline-related abbreviations, together with typical yield stress and yield strain values for common pipe barrel materials	32
5.1	PGA and Sa/g at 0.1 s values of six cities in Assam state	37

## LIST OF FIGURES

Figure Number	Description	Page Number
1.1	A map indicating the faults within a 500km radius of Guwahati city, including the Chedrang fault (CF), Churachandpur–Mao fault (CMF), and Dapsi thrust (DT)	2
1.2	Fire started in the Burhi Dihing river due to a pipe leak	3
1.3	The pipeline burst at RG Baruah Road, near Guwahati Commerce College	3
1.4	A blazing fire following a pipeline explosion in Sivasagar	3
1.5	Water pipeline at Kharguli Hill in Guwahati City explodes, injuring several people	3
1.6	Baghjan well blowout	3
1.7	Effect of landslide on pipeline	4
1.8	Locally buckled steel gas pipeline in the compression zone at North slope of Terminal Hill, 1994 Northridge earthquake	5
1.9	Beam buckling of water pipeline made of iron	5

<b>Figure Number</b>	<b>Description</b>	<b>Page Number</b>
1.10	Axial pull-out at the joint of a water supply pipeline at Tangshan East Water Works in Tangshan Earthquake 1976	6
1.11	A cast iron pipe at Navlakhi port failed during the 2001 Bhuj earthquake due to the breakdown of the bell-and-spigot joint, primarily caused by lateral spread	7
1.12	Flanged joint pipe failure	7
1.13	Water supply pipeline at Shippy Ghat, Port Blair, experienced a leak at the bell and spigot joint due to bending during the M9.0 Sumatra earthquake in 2004	8
1.14	Buckling of steel pipeline due to compressive forces during 1971 San-Fernando earthquake	9
1.15	Telescoped bell and spigot joint 48-inch weld steel pipe	9
1.16	Failure of pipe during 1999 Chi-Chi earthquake	10
3.10	Schematic diagram showing PGD due to soil failure	21
5.2	Shear wave velocity profile of the five different locations of Guwahati city	38

<b>Figure Number</b>	<b>Description</b>	<b>Page Number</b>
5.3	Strain vs Pipe thickness for pipe diameter 0.2 m	48
5.4	Strain vs Pipe thickness for pipe diameter 0.4 m	48
5.5	Strain vs Pipe thickness for pipe diameter 0.6 m	49
5.6	Strain vs Pipe thickness for pipe diameter 0.8 m	49

## CONTENTS

<b>Section</b>	<b>Title</b>	<b>Page Number</b>
Declaration		ii
Certificate		iii
Certificate from Head of the Department		iv
Acknowledgement		v
Abstract		vi
List of Tables		vii
List of Figures		viii
Chapter 1	Introduction	1-11
1.1	Seismic Risk to Pipelines in Assam	1
1.2	Mode of Pipeline Failure	4
1.3	Performance of Pipelines in Past Earthquakes	8
1.4	Soil Conditions of Guwahati City	10
1.5	Details of Pipelines Passing through Guwahati City	11
1.6	Objective of the Study	11

<b>Section</b>	<b>Title</b>	<b>Page Number</b>
Chapter 2	Review of Literature	12-15
2.1	General	12
2.2	Review of Literature	12
Chapter 3	Methodology	16-22
3.1	General	16
3.2	Scope	16
3.3	General Principles and Design Criteria	16
3.4	Classification of Pipeline	17
3.5	Classification of Seismic Hazard	17
3.6	Design Seismic Hazard	18
3.7	Analysis Procedure	18
3.8	Allowable Strain for Continuous Pipeline	20
3.9	Allowable Joint Displacement	21
3.10	Design Criteria for PGD	21
3.11	Design Criteria for Buoyancy	22
3.12	Design Criteria for Fault Crossing	22

<b>Section</b>	<b>Title</b>	<b>Page Number</b>
Chapter 4	Design Calculations	23-30
Chapter 5	Results and Discussion	31-40
Chapter 6	Geophysical Investigation	41-50
Chapter 7	Conclusion and Recommendations	51-52
References		53-55

## CHAPTER 1

# INTRODUCTION

---

### 1.1. Background

Pipelines are fundamental to modern infrastructure, offering reliable, economical, and efficient transportation of water, sewage, oil, natural gas, and other essential materials. Often termed "lifelines," these systems are vital for daily services and contribute significantly to the economic and social well-being of communities. Due to limited land availability and urbanization demands, buried pipelines are increasingly favored over above-ground alternatives.

The seismic safety of buried pipelines has become a critical concern due to their susceptibility to damage during earthquakes. Historical seismic events, such as the 1993 Latur earthquake, the 2001 Gujarat earthquake, the 2005 Kashmir earthquake, and the 2011 Sikkim earthquake, have shown that pipelines can endure substantial stresses during seismic activity, potentially leading to failures. Such failures can have severe repercussions, including contamination, water shortages, fires, and explosions, depending on the transported substance.

Assam, situated within the seismically active zone of the Indian Plate, faces significant seismic risks due to its complex tectonic setting. Active faults, such as the Oldham fault to the west of Guwahati and the Kopili fault to the east, have historically triggered powerful earthquakes, including the devastating 1897 Assam earthquake (Mw 8.1) and the 1923 Meghalaya earthquake (Ms 7.1) (Baro and Kumar, 2021). These events have highlighted the vulnerability of buried infrastructure in Assam, underscoring the urgent need to enhance the earthquake resilience of pipelines in the region.

Recent incidents in Assam further emphasize the importance of pipeline integrity in the face of seismic threats. For instance:

- In May 2023, a burst water pipe in Kharguli resulted in a fatality, injuries, and damage to approximately 30 houses and vehicles.
- In July 2023, an Oil and Natural Gas Corporation (ONGC) pipeline ruptured in Sivasagar, causing a crude oil spill.
- In July 2023, a burst water pipe in Silpukhuri, Guwahati, led to neighborhood flooding.

- In August 2023, a water pipeline in Maligaon, Guwahati, ruptured, leading to a significant water spill on the road.
- In August 2023, a water pipeline in Guwahati's Geetanagar neighborhood, installed by JICA, collapsed, raising concerns among residents.
- In December 2023, an explosion on Guwahati's Magazine VIP Road involving a gas pipeline injured three people.

These recent incidents, coupled with the seismic threat, highlight the necessity for implementing disaster risk reduction measures to mitigate potential consequences, including loss of life, property damage, and environmental concerns.

Understanding the behavior of buried pipelines under seismic excitation is crucial. Unlike above-ground structures, where inertia forces are the primary concern, buried pipelines are significantly influenced by the surrounding soil. The dynamic behavior of buried pipelines depends on various factors, including the type and frequency of incoming seismic waves, soil properties, pipeline material and dimensions, joint flexibility, and internal pressure. Additionally, more stress tends to accumulate at pipeline intersections compared to the remaining straight portions of the pipeline.



**Figure 1.2.** Fire started in the Burhi Dihing river due to a pipe leak. (Source- The Quint)



**Figure 1.3.** The pipeline burst at RG Baruah Road, near Guwahati Commerce College (Source- Rajesh Sharma, Twitter)



**Figure 1.4.** A blazing fire following a pipeline explosion in Sivasagar (Source- India Today)



**Figure 1.5.** Water pipeline at Kharguli Hill in Guwahati City explodes, injuring several people (Source- EastMojo)



**Figure 1.6.** Baghjan well blowout (Source- Hindustan Times)

## 1.2. Thesis Outline

Chapter 1 introduces the seismic risks faced by pipelines in Assam, including historical seismic events and recent incidents. It describes different modes of pipeline failure due to seismic activity and reviews the performance of pipelines during past earthquakes.

Chapter 2 summarizes the mechanisms of earthquake-induced ground movements and their interactions with buried pipelines.

Chapter 3 provides a detailed analysis of the behavior of buried pipelines subject to ground shaking. It explains the key factors influencing seismic action and pipeline vulnerability and presents a detailed review of existing pipeline fragility relations.

Chapter 4 summarizes common methods used to characterize site effects that influence ground shaking.

Chapter 5 presents the design calculations performed in the study, based on the IITK-GSDMA guidelines. It includes detailed examples of design calculations for different scenarios such as Permanent Ground Displacement (PGD), buoyancy due to liquefaction, fault crossing, and seismic wave propagation. The chapter also discusses the parametric studies conducted to evaluate strain variations in pipelines with different diameters and thicknesses.

Chapter 7 introduces geophysical methods such as Electrical Resistivity Tomography (ERT) and Ground Penetrating Radar (GPR) for monitoring the functioning of pipelines after installation and following seismic events. It describes the methodology, advantages, and applications of these methods for pipeline maintenance.

Chapter 8 summarizes the key findings of the study and their implications for the seismic resilience of buried pipelines. It provides practical recommendations for improving the seismic resilience of pipelines, including design guidelines and disaster risk reduction strategies.

References- This section lists all the references cited in the thesis.

## CHAPTER 2

# LITERATURE REVIEW

---

### 2.1. General

In this new chapter, a brief overview of relevant literature is presented, exploring the work done by various researchers on the vulnerability of buried pipelines and their seismic design.

### 2.2 Review of Literature

Bartlett and Youd (1995) presented empirical equations for predicting lateral spread displacement caused by liquefaction. Using a database of case histories from Japan and the United States, they developed multiple linear regression models to identify key parameters influencing lateral spread, including earthquake magnitude, distance to the seismic source, ground slope, and soil properties. Their empirical models provided practical tools for engineers to estimate lateral spread displacement and assess the seismic vulnerability of lifeline infrastructure. The study emphasized the importance of site-specific data for accurate predictions and highlighted the need for further research to refine the models.

Singh (2005) employs an integrated geophysical approach to investigate structural discontinuities and dislocations in the Kopili Valley, Assam Arakan Basin. Techniques such as seismic reflection and refraction, ERT, and GPR are used to map subsurface conditions. The research highlights the effectiveness of combining multiple geophysical methods for comprehensive subsurface mapping.

Hongjing, L.I. et al. (2008) presented a three-dimensional finite element model to analyze the response of buried pipelines under fault-induced permanent ground deformation. The model considered the interaction between the pipeline and surrounding soil, using nonlinear contact elements to simulate slip and isolation phenomena. The study investigated various influential factors, such as crossing angle, soil displacement, diameter-to-thickness ratio, friction coefficient, and burial depth. The findings indicated that larger crossing angles and deeper burial depths increased the seismic response of pipelines, while the optimal friction

coefficient for minimizing stress was around 0.3. This research provided valuable insights for the design and construction of earthquake-resistant pipelines.

Kaiser, A. E. et al. (2009) conducted high-resolution seismic reflection surveys across the Alpine Fault in New Zealand. Their study targeted fault zone structures in Holocene to late Pleistocene sediments. By employing innovative processing techniques, they produced detailed images of the fault zone, revealing a steep southeast dip of the fault through the Quaternary sediments. The study provided a provisional dip-slip rate of  $2.0 \pm 0.6$  mm/yr based on the vertical offset of the basement surface. These findings enhanced the understanding of the fault's geometry and behavior, contributing significantly to seismic hazard assessments in the region.

McClymont et al. (2009) investigated recent fault activity within the Taupo Rift of New Zealand using high-resolution 3-D ground-penetrating radar (GPR) data and trench-derived stratigraphic logs. They analyzed GPR data acquired over ten fault strands within the Maleme fault zone to determine slip accumulation patterns and rates. The study demonstrated that slip rates were variable over short time intervals, suggesting that multiple earthquakes were required for faults to exhibit uniform slip rates characteristic of their long-term behavior. The findings provided valuable insights into the spatial and temporal variability of fault displacement and the implications for seismic hazard assessment.

Mandal, et al. (2011) provided a detailed analysis of the seismic intensity scenario in Guwahati City, Assam. Using historical earthquake data and modern risk assessment tools, they generated intensity maps for various earthquake magnitudes. The study incorporated soil amplification factors derived from recent geotechnical investigations to estimate Peak Ground Acceleration (PGA) and Modified Mercalli Intensity (MMI) for different parts of the city. The findings revealed significant variations in seismic intensity across Guwahati, highlighting areas of high seismic risk. The paper emphasized the importance of site-specific seismic hazard assessments for effective urban planning and disaster management.

Solberg et al. (2011) focuses on mapping quick clay areas in mid Norway using a combination of geophysical and geotechnical methods. The research highlights the use of 2D resistivity measurements to distinguish between different types of clay deposits and to identify potential hazard zones. The study emphasizes the importance of integrating geophysical data with geotechnical investigations to provide a comprehensive understanding of subsurface conditions for hazard assessment and planning.

Mukherjee et al. (2013) investigated the seismic performance of buried continuous pipeline systems in Dehradun City, Uttarakhand, India. The study focused on the effects of different strain levels on the pipelines, considering both operational and seismic-induced strains. They conducted a parametric study to evaluate the impact of pipe diameter and installation depth on seismic performance. The analysis included four different earthquakes to generate near-field and far-field effects, using peak ground acceleration (PGA) values as input for computing axial strains due to seismic wave propagation. The study concluded that continuous pipeline systems in Dehradun City required site-specific seismic performance analysis, particularly for larger diameter pipes. The authors recommended minimizing burial depth in fault zones and avoiding abrupt changes in wall thickness within fault zones to reduce seismic risks.

Lanzano, et al. (2013) focused on the seismic vulnerability of industrial pipelines, particularly those used for transporting fluids such as water, oil, gas, and wastewater. Their study assessed the performance of continuous buried pipelines under seismic loading by analyzing observational data and deriving fragility curves. The authors classified the seismic damage into two categories: Strong Ground Shaking (SGS) and Ground Failure (GF). They introduced new fragility formulations based on the failure probability of pipelines, highlighting the importance of considering both transient and permanent ground deformations. The study emphasized the need for a multidisciplinary approach to evaluate the seismic behavior of pipelines, considering soil-structure interaction, material properties, and joint detailing. The findings provided critical insights for the seismic design and risk assessment of industrial pipelines.

Chenna, et al. (2014) examined the performance of a high-pressure gas pipeline in Gujarat under fault movement conditions. The study highlighted the importance of minimizing the burial depth of pipelines in fault zones to reduce soil restraint during seismic events. They discussed various seismic hazards affecting pipelines, including ground failure, ground motion, and other miscellaneous effects such as liquefaction and landslides. The paper emphasized the need for seismic design considerations in pipeline construction to ensure functionality during high-intensity earthquakes. The study provided recommendations for minimizing earthquake effects on existing pipelines, including design criteria for wave propagation, fault crossing, and permanent ground deformation (PGD).

Dash, et al. (2015) discussed the seismic vulnerability of pipelines in India, focusing on oil, gas, and water pipelines. They highlighted that many of India's pipelines traverse high seismic zones, posing significant risks. The paper reviewed the performance of pipelines during past Indian earthquakes, such as the 1999 Chamoli earthquake and the 2001 Gujarat earthquake. It emphasized the need for robust seismic design and mitigation techniques to prevent pipeline failures during future earthquakes. The study also provided a comprehensive overview of existing and proposed pipeline networks in India, along with their seismic risk profiles.

McClymont et al. (2016) demonstrates the integration of geophysical and geotechnical methods to assess pipeline geohazards. The study presents case studies where electrical resistivity tomography (ERT), seismic refraction tomography (SRT), and ground-penetrating radar (GPR) were used to characterize subsurface conditions along proposed pipeline routes. The research highlights the effectiveness of combining multiple geophysical techniques to obtain detailed subsurface information, which aids in optimizing borehole locations and improving geohazard assessments.

Haque, et al. (2019) provided a comprehensive review of the seismic behavior of buried pipelines. They discussed the differences between the behavior of buried pipelines and above-ground structures during seismic events, emphasizing the importance of soil-pipe interaction. The review categorized pipeline damage into transient ground deformation (GDt) and permanent ground deformation (GDp), highlighting various failure modes such

as shell mode buckling, beam mode buckling, tensile failure, and cross-section ovalization. The paper also reviewed existing modeling techniques, including beam on elastic foundation, shell models, plane-strain models, and hybrid models. The authors identified research gaps and proposed areas for further study, such as the need for more advanced three-dimensional numerical analyses and the consideration of fault movement and soil liquefaction effects.

Gawande, et al. (2019) investigated the response of buried steel pipelines subjected to strike-slip fault movements using finite element analysis (FEA). They considered the interaction between the pipeline and the surrounding soil, accounting for contact nonlinearity, material nonlinearity, and geometrical nonlinearity. The pipeline material was API X65 grade steel, modeled using J2 plasticity theory with strain-hardening. The research focused on the onset of buckling-mode failure under varying conditions such as pipe diameter-to-thickness ratios, internal pressure, fault displacement, and fault offset rates. Key findings included that higher diameter-to-thickness ratios increased fault resistance, lower internal pressure enhanced fault resistance, and fault resistance increased with higher fault offset rates. The study identified pre-buckling patterns and the conditions leading to buckling failure. The results provided insights into the mechanical behavior of pipelines during seismic events and offered guidelines for designing earthquake-resistant buried pipelines.

Baro, et al. (2019) employed a probabilistic seismic hazard analysis (PSHA) to assess seismic hazards in the Shillong Plateau (SP), focusing on highly populated districts such as Shillong, Nongpoh, and Tura. The analysis used historical and instrumentally recorded earthquake data to address uncertainties related to earthquake magnitudes, rupture locations, and ground motion exceedance. The study identified the Barapani fault as having the highest frequency of seismic hazard for Shillong and Nongpoh, while the Eocene hinge zone and Dauki faults posed significant risks for Tura. The results provided valuable information for engineering applications and disaster risk management in the region.

Baro and Kumar (2021) examined the seismic vulnerability of oil and gas pipelines in Guwahati City, Assam. The pipelines, which transport crude oil, petroleum products, and natural gas, traverse several tectonically active faults, including the Oldham, Kopili, and

Dhubri faults. These faults have historically generated significant earthquakes, such as the 1897 Assam earthquake (Mw 8.1) and the 1930 Dhubri earthquake (Ms 7.1). The study highlighted that since the pipelines were laid post-1962, no major earthquakes have occurred, leaving their seismic vulnerability largely untested. The review aimed to understand the potential impacts of future seismic events on these pipelines and the consequent risks to the inhabitants of Guwahati.

Butchibabu et al. (2021) aims to protect a crude-oil pipeline buried at a shallow depth against environmental hazards and pilferage. The research employs surface and borehole geophysical techniques, including ERT, GPR, SRT, cross-hole seismic tomography (CST), and cross-hole seismic profiling (CSP), to map vulnerable zones. The integrated geophysical investigations revealed the presence of voids, cavities, and weak zones below the pipeline, which were critical for assessing pipeline stability and planning remedial measures.

Raghavendra and Baro (2022) aimed to understand and quantify the liquefaction-induced lateral spreading potential of Guwahati city soil. They used contour maps from previous studies to identify sites with high liquefaction potential and classify them based on sub-soil properties, layer thickness, fines content, groundwater table depth, ground slope, earthquake magnitude, and source-to-site distance. A Multiple Linear Regression (MLR) model was employed to estimate displacement lengths, which ranged from 0.02m to 0.11m. The study highlighted the importance of understanding the lateral spreading potential to mitigate the risks associated with future earthquakes in Guwahati.

Bandyopadhyay, et al. (2022) presented a probabilistic seismic hazard assessment (PSHA) for the Assam region, incorporating site-specific amplification studies. The study area was divided into ten areal zones based on seismicity source modeling. Earthquake recurrence parameters were obtained from the Gutenberg–Richter recurrence relation using an updated earthquake catalog from 1735 to 2021. Hazard curves were generated using a logic tree structure to minimize epistemic uncertainty. The peak ground acceleration (PGA) values for different return periods were provided, and site-specific response spectra for major cities in Assam were proposed. The study also included a site amplification study for Guwahati, providing surface-level response spectra for different earthquake return periods.

Inocente, et al. (2023) assessed the earthquake damage to buried pipeline networks in the Lima Metropolitan Area (LMA), Peru. They performed a deterministic seismic hazard analysis for an inter-plate earthquake scenario, using ground motion prediction equations and site conditions to compute peak ground velocity (PGV) distribution. Empirical fragility functions were selected to estimate pipeline repair ratios and total repairs for the scenario. The study highlighted the importance of using appropriate fragility functions and provided a logic tree for their selection. The results were geographically presented using a GIS, offering valuable insights for emergency response and risk mitigation in the LMA.

Borah, M. et al. (2024) presented a comprehensive seismic hazard assessment for Assam, incorporating site-specific studies and a probabilistic approach. The study divided the North-East India region into ten seismic source zones based on seismicity and tectonics. Using an updated earthquake catalog from 1897 to 2022, they calculated seismicity parameters and employed a topography-based Vs30 model for ground motion prediction equations (GMPEs). The hazard maps for Assam were prepared in terms of peak ground acceleration (PGA) and spectral acceleration (Sa) values. The study also included ground response analysis for Guwahati, showing significant amplification of surface-level PGA values. The results provided valuable insights for seismic hazard mitigation and structural design in Assam.

Bhadran, A et al. (2024) presented a multi-model seismic susceptibility assessment for the 1950 Great Assam earthquake, focusing on the Eastern Himalayan front. They employed various multi-criteria decision-making (MCDM) methods, including Analytical Hierarchy Process (AHP), Fuzzy-AHP (FAHP), and Maximum Entropy (MaxEnt), to determine seismic susceptibility. The authors assigned weightage to nine controlling factors such as predominant frequency, geology, vulnerability index, peak amplification, liquefaction potential, groundwater condition, shear wave velocity (Vs30), peak ground acceleration (PGA), and land use/land cover. The MaxEnt model exhibited the highest accuracy (87.5%) when compared using the receiver operating characteristic curve (ROC) and area under the curve (AUC) value. The study highlighted the importance of integrating various models to improve seismic risk mitigation strategies and aid urban planners in designing earthquake-resistant buildings.

## **2.3 Objectives**

- i. **Assess Seismic Vulnerability of Buried Pipelines:** Evaluate the condition, vulnerabilities, and historical performance of Guwahati City's pipeline network in earthquake-prone regions.
- ii. **Utilize IITK-GSDMA Guidelines:** Apply the IITK-GSDMA guidelines to design and assess the seismic resilience of buried pipelines in Guwahati.
- iii. **Develop a Practical Tool:** Formulate an Excel sheet based on IITK-GSDMA guidelines, incorporating site-specific data for Guwahati derived from previous earthquake data and literature.
- iv. **Conduct Parametric Studies:** Analyze the variations in strain for different pipe diameters and thicknesses under seismic loading conditions.
- v. **Enhance Disaster Risk Reduction:** Provide a holistic and effective strategy for disaster risk reduction through improved seismic resilience of water supply infrastructure in Assam.

# EARTHQUAKE EFFECTS AND PIPELINE BEHAVIOUR

---

### 3.1. Effects of Earthquake

The impact of earthquakes on buried pipelines is best understood by examining the displacements induced in the surrounding soil. Earthquakes cause both direct effects, such as surface faulting and ground shaking, and indirect effects, including liquefaction, landslides, soil densification, and tsunamis.

The primary way earthquakes affect buried pipelines is through the displacements they cause in the surrounding soil. Damage can occur due to Transient Ground Deformation (GDt) or Permanent Ground Deformation (GDp), or a combination of both. GDp involves irreversible ground movement due to ground failure or strain, while GDt involves soil movement and strains caused by strong shaking. Although GDt can cause ground cracks, its residual deformation is usually less than its maximum during shaking.

The severity of these effects on buried pipelines varies depending on the earthquake. Transient effects are common and spread over large areas, causing widespread but relatively low rates of pipeline damage. In contrast, surface fault rupture and collateral earthquake effects can lead to high ground strains where pipelines are located, resulting in localized but potentially severe pipeline damage.

#### 3.1.1 *Faulting*

Most earthquakes occur due to the accumulation of stress at tectonic plate boundaries. When these stresses surpass the rock's strength, a rupture happens along a fault line, releasing the stored strain energy as seismic waves and heat. Fault ruptures generally occur along pre-existing fractures in the Earth's crust. The extent of faulting is closely related to the earthquake's magnitude, with larger earthquakes capable of producing faults that span several hundred kilometers in length, tens of kilometers in width, and several meters in offset.

Faults are classified based on the relative movement of their sides. Horizontal movement predominantly characterizes strike-slip faults. Dip-slip faults feature movement mainly in the direction of the fault plane's dip. When the horizontal component of a dip-slip fault is compressional, it is termed a Reverse Fault; if it is extensional, it is called a Normal Fault. Faults with both dip-slip and strike-slip movements are known as Oblique Faults.

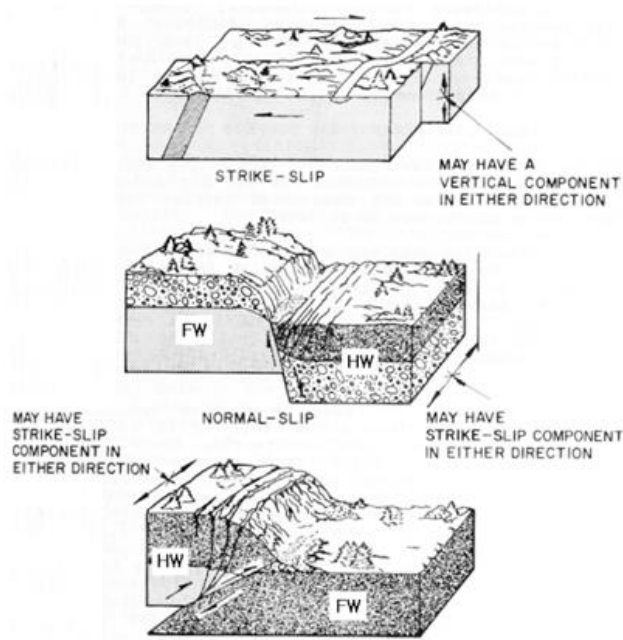


**Figure 3.1.** Surface expression of different type of faulting (Taylor and Cluff, 1977)

Extensive research has investigated the relationship between earthquake magnitude and fault rupture characteristics. Wells and Coppersmith (1994) compiled a global database of 244 earthquakes, with moment magnitudes ranging from 5.6 to 8.1. They found that fault displacements ranged from 0.05 to 8.0 meters for strike-slip faults, 0.08 to 2.1 meters for normal faults, and 0.06 to 1.5 meters for reverse faults. Using this data, they derived empirical relationships among magnitude, rupture length, rupture width, rupture area, and surface displacement.

Where,  $D$  = average surface fault displacement (m),

$M_w$  = moment magnitude,

$C_1, C_2$  = coefficients derived from the regression

$$\log \bar{D} = C_1 + C_2 M_w \quad (3.1)$$

Values for different categories of fault slip type are in Table 3.1.

**Table 3.1** Regression coefficients for different categories of Fault slip type  
(Wells & Coppersmith, 1994)

Fault slip type	C1	C2	Standard Deviation	Correlation Coefficient	Magnitude range
Strike-slip	-6.32	0.90	0.28	0.89	5.6 - 8.1
Reverse	-0.74	0.08	0.38	0.10	5.8 - 7.4
Normal	-4.45	0.63	0.33	0.64	6.0 - 7.3
All	-4.80	0.69	0.36	0.75	5.6 - 8.1

The behavior of a buried pipeline in response to surface faulting is significantly influenced by its alignment relative to the fault. Potential responses include bending, buckling from axial compression, or pull-out from axial extension. Dip-slip faulting generally causes more damage to pipelines than strike-slip faulting for similar ground displacements. This is because the bearing pressure on an object moving downward through soil is greater than the lateral resistance to movement. Analytical models detailing the behavior of buried pipelines under earthquake faulting conditions are discussed in O'Rourke & Liu (1999).

### 3.1.2 *Ground Shaking*

Ground shaking results from two types of seismic waves: body waves and surface waves. Both are crucial when assessing the response of buried pipelines to seismic activity. S-waves, a type of body wave, are primarily considered due to their higher energy compared to P-waves. Among surface waves, R-waves are most significant as they induce axial strains in pipelines, which are more critical than the bending strains caused by L-waves (O'Rourke & Liu, 1999).

Analytical models of soil-pipeline interaction and field data on strong-motion suggest that body waves and surface waves impact buried pipelines differently. For accurate prediction of earthquake damage to pipeline systems or designing earthquake-resistant pipelines, it is essential to identify the predominant wave effects at a specific site or region.

Nakamura (1988) established criteria for determining the dominance of surface waves at a site based on earthquake magnitude ( $M$ ), focal depth ( $h$ ), and epicentral distance ( $d_e$ ). Kamiyama et al. (1992) applied these criteria to differentiate between conditions where body waves or surface waves are likely to predominate.

Conditions for domination of surface waves are given by the expressions below:

$$M > 6.0 \text{ and } \frac{d_e}{h} > 1.5 \quad (3.2)$$

$$6.0 \geq M > 5.0 \text{ and } \frac{d_e}{h} > 6.0 \quad (3.3)$$

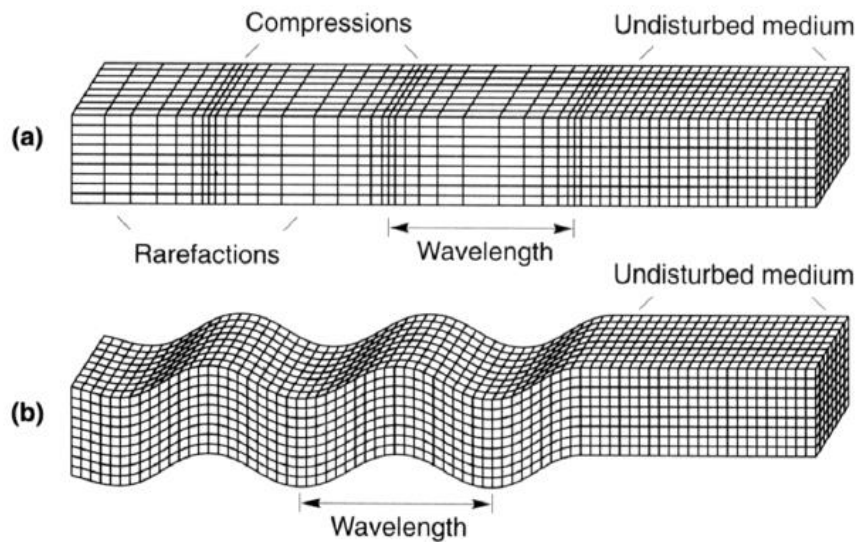


**Figure 3.2.** Deformation produced by body waves (a) P-wave, (b) SV (Vertical)- wave (Bolt,1993)

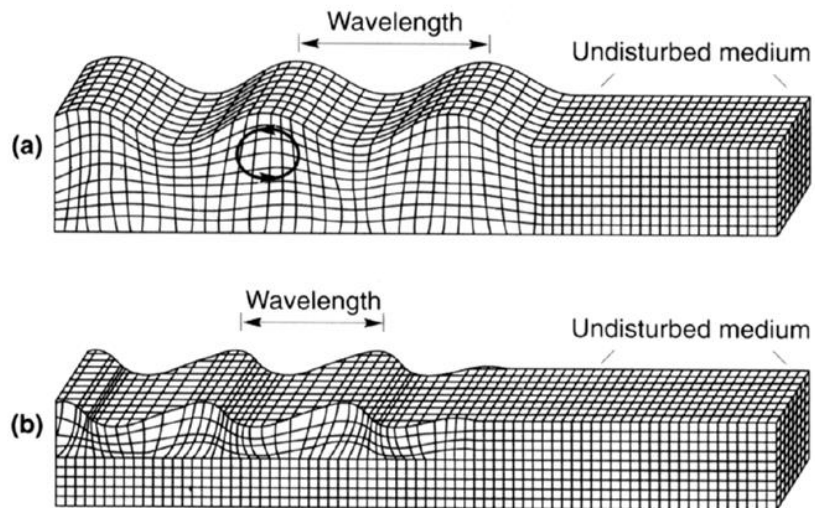


**Figure 3.3.** Deformation produced by surface waves (a) R-wave, (b) L-wave (Bolt,1993)

The response of buried pipelines to seismic waves differs substantially from that of most above ground structures.

A fluid-filled pipeline typically has less weight than the soil it replaces. Inertial forces are therefore low with respect to the stiffness of the surrounding soil. The response of the pipeline to ground shaking depends on the level of strain induced in the ground, the stiffness of the soil, the stiffness of the pipeline and the frictional resistance at the pipeline-soil Interface.

### 3.1.3 *Strong-motion Parameters*

For earthquake engineering applications, key strong-motion characteristics include amplitude, duration, frequency content, and energy.

#### a) Amplitude Parameters

The most common measure of earthquake motion amplitude is the Peak Ground Acceleration (PGA). While accelerations are directly related to inertial forces, PGA is not a particularly accurate indicator of structural damage. For pipelines, regions of high PGA have been associated with damage primarily due to permanent ground deformations (O'Rourke & Toprak, 1997).

Peak Ground Velocity (PGV) is less sensitive to high-frequency components of ground motion and is therefore a useful indicator of the effects of ground motion on structures like tall or flexible buildings that are sensitive to intermediate frequencies. Peak ground displacements (PGD) relate more to the low-frequency content of strong ground motion. When displacements are calculated from integrated acceleration time-histories, their reliability in characterizing true ground motion is limited by raw data processing inaccuracies and long-period noise.

#### b) Duration Parameters

The duration of strong ground motion significantly influences the level of earthquake damage. In specific ground conditions, such as liquefiable deposits, repeated moderate amplitude stress or load cycles over an extended period can cause more damage than higher amplitude motion over a shorter duration.

#### c) Frequency-Content Parameters

The frequency content of input motion significantly affects the earthquake response of structures and the ground. For buried structures, the response of the soil layers in which they are embedded is sensitive to frequency content. Thus, it is crucial to consider how ground motion amplitude is distributed across different frequencies. Response and Fourier spectra plots are commonly used to identify dominant ground motion components that might significantly influence the response of certain structures or soil types.

The response spectrum describes the maximum response of a single-degree-of-freedom (SDOF) system to a given input motion, considering the natural frequency (or natural period) and damping ratio of the SDOF system. This response can be expressed in terms of displacement, velocity, or acceleration, with the maximum response values

referred to as spectral displacement (SD), spectral velocity (SV), and spectral acceleration (SA), respectively. Spectral acceleration at zero natural period (corresponding to an infinite natural frequency) is equal to PGA.

The peak velocity and peak acceleration values relate to the high and intermediate frequency components of strong ground motion, respectively. The PGV/PGA ratio measures the relative importance of these frequency ranges in the motion. For simple harmonic motion,  $(PGV/PGA)^2$  equals the period, T. This quantity for multi-frequency content motion can provide a measure of the effective period of the ground motion (Tso et al., 1992; Kramer, 1996).

## 3.2. Collateral Effects

### 3.2.1 Liquefaction

Liquefaction refers to a range of complex soil deformation phenomena characterized by the generation of excess pore-water pressure under undrained loading conditions. Historical earthquakes have shown that liquefaction can cause significant damage to both above-ground and buried structures. Past events have demonstrated that liquefaction-induced damage can severely impact buried lifelines, making the zonation of liquefaction hazard crucial for lifeline earthquake engineers. Not all soils are prone to liquefaction, so the first step in evaluating liquefaction hazard is to determine the soil's susceptibility.

Liquefaction susceptibility for any given soil can be assessed based on various historical, geological, compositional, or soil state criteria. Once it is established that a soil has the potential for liquefaction, the next step is to assess the likelihood that an earthquake will generate strong enough shaking to trigger this phenomenon. The criteria for liquefaction susceptibility and the conditions required to trigger it are intricate and beyond the scope of this discussion.

For instance, Hamada et al. (1986) developed a formula to predict horizontal ground displacement caused by liquefaction-induced lateral spreads, using data from the 1964 Niigata and 1983 Nihonkai-Chubu earthquakes. By comparing pre- and post-earthquake aerial photographs, they identified ground deformation patterns and divided lateral spreads into discrete blocks. They then averaged the horizontal displacement, thickness of the liquefied layer, and ground slope severity within each block to create a predictive expression.

$$D_H = 0.75\sqrt{H_{liq}}^3\sqrt{\theta} \quad (3.4)$$

Where,  $D_H$  = Horizontal ground displacement (m),  
 $H_{liq}$  = Thickness of the liquefied layer (m),  
 $\theta$  = Maximum of slope of base of liquefied layer and slope of ground surface (%)

$H_{liq}$  is a parameter which indirectly accounts for the amount of ground shaking (a function of earthquake magnitude and distance) as well as the soil conditions at the site.

### 3.2.2 Landslides

In many earthquakes, the economic and social impact of landslide damage has often exceeded that of all other seismic hazards combined (Kramer, 1996). Landslides encompass a wide range of gravity-driven movements of earth materials downslope, generally classified into three main categories: disrupted slides and falls, coherent slides, and lateral spreads and flows.

**Disrupted Slides and Falls:** These are the most catastrophic types of failures, occurring in steep terrain and characterized by high velocities. They involve sudden and rapid movements of earth materials, making them particularly dangerous.

**Coherent Slides:** These typically involve deep-seated translational movements of blocks of intact material sliding along a basal shear surface. Occurring on moderate to steep slopes, coherent slides generally move at much lower velocities than disrupted slides.

**Lateral Spreads and Flows:** These are translational movements on basal zones of liquefied gravel, sand, silt, or weakened sensitive clay. More disrupted than soil slumps or block slides, lateral spreads contain many internal fissures and grabens. Rapid soil flows exhibit fluid-like behavior and can involve large volumes of soil traveling significant distances.

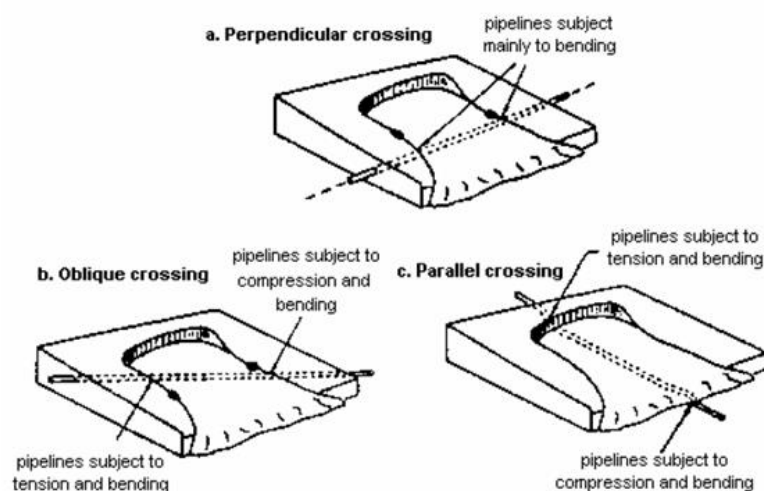


**Figure 3.4.** Principle effects of landslides on pipeline as per orientation (O'Rourke, 1998)

Studies of past earthquakes have shown the relative abundance of different types of landslides across a broad range of earthquakes and geological environments. This provides a global indication of the relative importance of each hazard to the built environment, as more frequent types of landslides are more likely to cause damage to engineered structures. However, the prevalence of each landslide type can vary significantly between earthquakes.

Buried pipelines are particularly vulnerable to differential movements in the surrounding soil. The extent, amount, and abruptness of permanent ground deformation associated with a landslide will influence the degree of pipeline damage. The interaction between soil and pipe is primarily affected by the stiffness of the soil. Therefore, zonation of landslide hazards is a critical step in identifying vulnerable sections of pipeline system.

### 3.2.3 *Densification*

Earthquake-induced strong ground shaking can lead to the densification of both cohesive and cohesionless soils, resulting in ground surface settlement, which poses significant risks to buried infrastructure (O'Rourke & Liu, 1999).

Takada & Tanabe (1988) developed formulae to estimate ground settlement during earthquakes through regression analysis of 404 instances of ground settlement from five major Japanese earthquakes ( $7.4 \leq \text{MJMA} \leq 7.9$ ). These expressions were specifically designed for earthquake-resistant lifeline facilities, driven by the high levels of settlement-induced pipeline damage observed in these earthquakes. Two expressions are provided: one for the settlement of an embankment ( $\delta_1$ ) and another for the settlement of a plain (level) site ( $\delta_2$ ). Both  $\delta_1$  and  $\delta_2$  are measured in centimeters.

$$\delta_1 = \frac{C_1 B H_{\text{sand}} a_p}{N_{\text{SPT}}} + C_2 \quad (3.5)$$

$$\delta_2 = \frac{C_3 H_{\text{sand}} a_p}{N_{\text{SPT}}} + C_4 \quad (3.6)$$

Where,

B = embankment height (m),

$H_{\text{sand}}$  = thickness of the sandy layer (m),

$N_{\text{SPT}}$  = Standard Penetration Test (SPT) N-value of the sandy layer,

$a_p$  = PGA (in  $\text{cm/s}^2$ ),

$C_i$  = coefficients of regression.

$C_1$  has dimensions of  $\text{s}^2/\text{m}^2$ ;  $C_2$  and  $C_4$  have dimensions of cm;  $C_3$  has dimensions of  $\text{s}^2/\text{m}$ .

These coefficients were derived for two different datasets: settlements in liquefied soil, and settlements in both liquefied and non-liquefied soil.

**Table 3.2** Regression coefficients for calculation of  $\delta_1$  and  $\delta_2$

Quantity Predicted	Type of site	Dataset	C1	C2	Correlation coefficient	Size of dataset
$\delta_1$	Embankment	Liquified Soil	0.123	19.3	0.88	35
$\delta_1$	Embankment	Liquified and non-liquified soil	0.118	19.9	0.88	42
Quantity Predicted	Type of site	Dataset	C3	C4	Correlation coefficient	Size of dataset
$\delta_2$	Plain Site	Liquified Soil	0.339	3.79	0.81	41
$\delta_2$	Plain Site	Liquified and non-liquified soil	0.332	4.86	0.82	43

The expressions indicate that ground settlement increases with the thickness of the sandy soil layer and with PGA but decreases with increasing SPT N-value of the sandy layer. Settlements in liquefied soil were greater than settlements in non-liquefied soil, all other factors being equal. No ground settlement was observed for PGA below 50 cm/s<sup>2</sup>.

### 3.3. Performance of Pipelines in Past Earthquakes

- a) **1971 San Fernando Earthquake ( $M_w - 6.6$ ):** The seismic event caused direct losses, damaging a 1.24 m water pipeline and welded joints at Nine Bend. Ductile steel pipelines withstood ground shaking but failed due to deformation from faulting. Eleven transmission pipelines suffered damage from liquefaction-induced lateral spread and landslides, with 80 breaks occurring in the upper San Fernando Valley, mainly in an old oxyacetylene-welded section, attributed to compressive forces causing pipe wrinkling.
- b) **1994 Northridge Earthquake ( $M_w - 6.7$ ):** The event resulted in approximately 1,400 pipeline breaks in the San Fernando Valley, with a dispersed pattern outside high liquefaction zones attributed to old brittle pipes damaged by ground movement. On Balboa Boulevard, a 0.5588m pipe suffered two breaks, one in tensile and the other in compressive failure, located in a ground rupture zone perpendicular to the pipeline. Leaking gas ignited at various locations, and broken water and gas lines experienced 0.1524 to 0.3048 m of separation. Widespread ground cracking and differential settlements occurred, with a sewage pipe rupturing at Jensen Filtration.
- c) **1999 Chi-Chi Earthquake ( $M_w - 7.7$ ):** In Taiwan, numerous water and gas pipelines were damaged at various locations. Gas pipelines experienced bending deformation near the

Wushi Bridge, around 10 km south of Taichung, due to ground displacement at a reverse fault.

- d) **1988 Bihar Earthquake ( $M_w - 6.6$ ):** A majority of the water pipelines in the Andaman and Nicobar Islands suffered severe damage, whereas the oil pipelines demonstrated better resilience. Instances of breakages occurred primarily at the junctions where pipes connected with facilities such as tanks and machines.
- e) **1999 Chamoli Earthquake ( $M_w - 6.8$ ):** The pipelines supplying water to Chamoli and Gopeshwar towns experienced disruptions caused by landslides, leading to damages.
- f) **2001 Gujarat Earthquake ( $M_w - 7.7$ ):** The majority of liquid fuel facilities remained unaffected. However, some damage occurred at the points where pipelines connected to equipment at pump stations.
- g) **2004 Sumatra Earthquake ( $M_w - 9$ ):** A significant portion of water pipelines in the Andaman and Nicobar Islands sustained severe damage, while the oil pipelines demonstrated greater resilience. Instances of breakages occurred at pipe junctions connected to facilities such as tanks and machines.
- h) **1897 Assam Earthquake ( $M_s - 8.7$ ):** The 1897 Assam earthquake, one of the most powerful earthquakes in the Indian subcontinent, caused extensive damage to infrastructure in Assam and Meghalaya. The earthquake's intensity and ground shaking resulted in significant ground deformation, including fissures and sand vents. The impact on buried pipelines was likely severe, particularly at junctions and connection points.
- i) **1923 Meghalaya Earthquake ( $M_s - 7.1$ ):** The 1923 Meghalaya earthquake caused heavy damage in Mymensingh, Cherrapunji, and Guwahati. The earthquake's intensity and ground shaking likely affected buried pipelines in these areas. The earthquake's impact on buildings and infrastructure highlights the potential vulnerabilities of pipeline systems to seismic activity.
- j) **1930 Dhubri Earthquake ( $M_s - 7.1$ ):** It caused extensive damage to buildings and infrastructure in western Assam. The earthquake's early morning occurrence and strong shaking likely affected buried pipelines, particularly at junctions and connection points of pipeline. The earthquake's impact extended to Kolkata, Chittagong, Dibrugarh, and Patna, indicating a widespread effect on infrastructure.
- k) **1943 Hojai Earthquake ( $M_s - 7.2$ ):** The Hojai earthquake caused significant ground shaking in northeast India. The earthquake's impact on the Manipur Road and surrounding areas suggests potential vulnerabilities in pipeline systems.

- l) **1950 Assam Earthquake ( $M_w - 8.7$ ):** The 1950 Assam earthquake, one of the largest earthquakes in the 20th century, caused widespread devastation in Upper Assam. The earthquake resulted in significant ground deformation, including fissures and sand vents, which likely affected buried pipelines. The region experienced severe flooding due to landslides damming tributaries of the Brahmaputra River, further complicating the impact on pipeline infrastructure.
- m) **1984 Silchar Earthquake ( $M_w - 6.0$ ):** It resulted in moderate damage to water pipelines in the affected areas. The Sonaimukh bridge over the Sonai River was dislodged from its abutment, and several school buildings with traditional Assam-type construction were severely damaged. The earthquake caused numerous cracks in the floor and walls of structures, indicating potential vulnerabilities in the pipeline infrastructure.

### 3.4. Modes of Pipeline Failure

#### 3.4.1. Continuous Pipeline

A continuous pipeline is a network of pipes that are connected without any breaks or interruptions. It allows for the smooth and uninterrupted flow of liquids, gases, or other substances from one place to another.

##### a) Tensile Failure

Tensile strain in the pipeline may occur because of seismic hazards like faulting, landslides, liquefaction, and relative ground motion at pipe supports. Figure 3.5 demonstrates how a landslide can lead to the pipeline experiencing significant tensile strain.

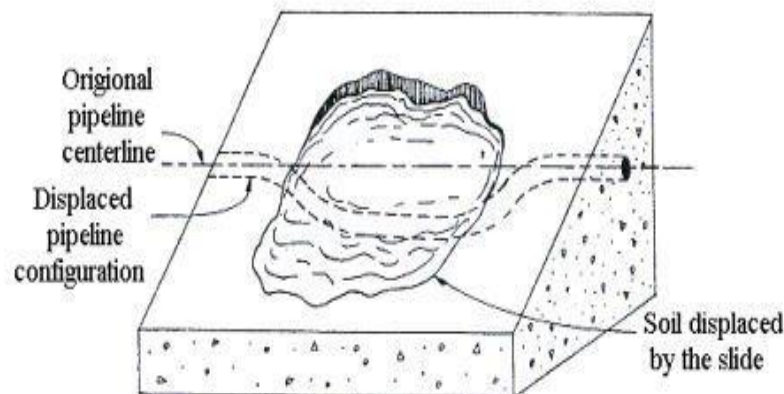


**Figure 3.4.** Effect of landslide on pipeline resisting tensile strain (ASCE, 1984)

### **b) Local Buckling**

Buckling or wrinkling in pipelines can occur when a specific part of the pipe wall becomes unstable. Once this wrinkling starts, any further movement in the ground tends to focus on these wrinkles, causing the pipe wall to curve and eventually crack, leading to leaks. This is a common issue with steel pipes. Figure 3.5 shows an example of this happening to a 77-inch welded steel pipe during the 1994 Northridge earthquake.



**Figure 3.5.** Locally buckled steel gas pipeline in the compression zone at North slope of Terminal Hill, 1994 Northridge earthquake (EERI, 1995)

### **c) Beam Buckling**

The beam buckling of a pipeline is similar to how a slender column might buckle, like Euler buckling. In this case, the pipe experiences an upward displacement. Unlike local buckling, where strain concentrates in one area, beam buckling spreads the relative movement over a larger distance. This results in less significant compressive strains in the pipeline and reduces the risk of tearing the pipe wall. Beam buckling is considered more preferable, especially in ground compression zones. It typically occurs in pipelines buried at shallow depths, around 3 feet or less. This can also happen during intentional post-earthquake excavations designed to relieve compressive strain in the pipes. Figure 3.6 illustrates beam buckling in an iron water pipeline during the M7.8 San Francisco earthquake in 1906.



**Figure 3.6.** Beam buckling of water pipeline made of iron.  
(USGS Photo Library)

### **3.4.2. Segmented Pipeline**

A segmented pipeline refers to a system of pipes that is divided or broken into distinct sections or segments rather than being continuous or unbroken. These segments may have joints or connections between them, allowing for easier installation, maintenance, or replacement of specific portions of the pipeline without affecting the entire system.

#### **a) Axial Pull-out**

In regions where the ground experiences tensile strain, a typical failure mode for a segmented pipeline is axial pull-out at joints. This occurs because the shear strength of the joint caulking material is significantly lower than that of the pipe. Figure 3.7 illustrates a 30cm diameter cast iron pipeline being pulled apart by 25cm during the 1976 Tangshan earthquake.



**Figure 3.7.** Axial pull-out at the joint of a water supply pipeline at Tangshan East Water Works in Tangshan Earthquake 1976 (EERL, 2004)

### b) Crushing of bell-and-spigot joints

In places where the ground is under compressive strain, a common way segmented pipelines fail is by the bell-and-spigot joints getting crushed. Figure 3.8 displays an example of a cast iron pipe failing because the bell-and-spigot joint broke during the Bhuj earthquake on January 26, 2001, in the Navlakhi port area.



**Figure 3.8.** A cast iron pipe at Navlakhi port failed during the 2001 Bhuj earthquake due to the breakdown of the bell-and-spigot joint, primarily caused by lateral spread (ASCE, 2001).

### c) Flanged joint failure

In regions experiencing tensile ground strain, a pipeline with flanged joints can fail at the joint when the flange connection breaks. Figure 3.9 illustrates a failure of a flanged joint pipe due to elevated tensile strain.



**Figure 3.9.** Flanged joint pipe failure (ASCE,1997)

### d) Circumferential flexural failure and joint rotation

When a segmented pipeline bends due to ground movement or seismic shaking, joints rotate and pipe segments flex to accommodate the curvature. The balance between joint rotation and pipe flexure depends on their stiffness. Figure 3.10 shows a pipeline leaking at a joint due to excessive bending in the 2004 Sumatra earthquake.



**Figure 3.10.** Water supply pipeline at Shippy Ghat, Port Blair, experienced a leak at the bell and spigot joint due to bending during the M9.0 Sumatra earthquake in 2004 (Photo: Suresh R Dash).

**BURIED PIPELINE RESPONSE**

**5.1. Ground and pipe strain induced by earthquake**

To assess the impact of seismic wave propagation on buried pipelines, quantifying ground strain is crucial. When seismic excitation at the surface is modeled as a simple traveling wave with a consistent shape, it can be demonstrated that the peak horizontal soil strain ( $\epsilon_p$ ) in the propagation direction is connected to the peak horizontal particle velocity ( $v_p$ ) in the same direction through the relationship (Newmark, 1967 and Rosenblueth, 1971)

$$\epsilon_p = \frac{v_p}{c} \tag{4.1}$$

Where,  $c$  = apparent propagation velocity of wave w.r.t. the ground surface

Equations (4.3), (4.5), and (4.7) in Table 4.1 provide the maximum longitudinal strain along with the corresponding value of  $\epsilon$ . For P-waves and R-waves, the maximum longitudinal strain is observed when the propagation direction is parallel to the axis of pipe. In the case of S-waves, the maximum strain occurs when the propagation direction is oblique to the pipeline axis ( $\phi = 45^\circ$ ).

**Table 4.1** Ground strain induced by seismic waves (along a pipeline) (St. John & Zahrah, 1987)

Wave Type	Longitudinal strain	Maximum longitudinal strain
P-wave	$\epsilon = \frac{V_{pP}}{c_p} \cos^2 \phi$ (4.2)	$\epsilon = \frac{V_{pP}}{c_p}$ for $\phi = 0^\circ$ (4.3)
S-wave	$\epsilon = \frac{V_{pS}}{c_s} \sin \phi \cos \phi$ (4.4)	$\epsilon = \frac{V_{pS}}{2c_s}$ for $\phi = 45^\circ$ (4.5)
R-wave	$\epsilon = \frac{V_{pR}}{c_R} \cos^2 \phi$ (4.6)	$\epsilon = \frac{V_{pR}}{c_R}$ for $\phi = 0^\circ$ (4.7)

Where,

- $V_{pP}$  = peak particle velocity caused by P-waves
- $c_p$  = apparent P-wave propagation velocity
- $V_{pS}$  = peak particle velocity caused by S-waves
- $c_s$  = apparent S-wave propagation velocity
- $V_{pR}$  = peak particle velocity caused by R-waves
- $c_R$  = apparent R-wave propagation velocity
- $\phi$  = angle of incidence of wave w.r.t. tunnel axis

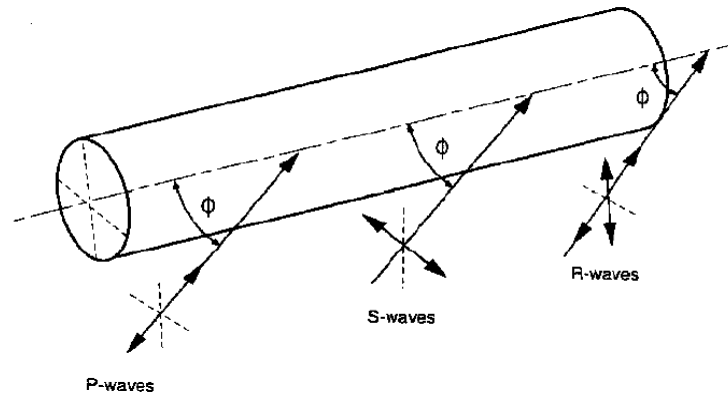


**Figure 4.1.** Angle of incidence of seismic wave w.r.t. to axis of pipeline (Hashash et al., 2001)

The variation in PGV values with depth, observed from downhole array, is generally not that significant for typical buried pipeline depths (0.5-3 m) (Tromans, 2004).

#### 4.1.1. Ground strain caused by body waves

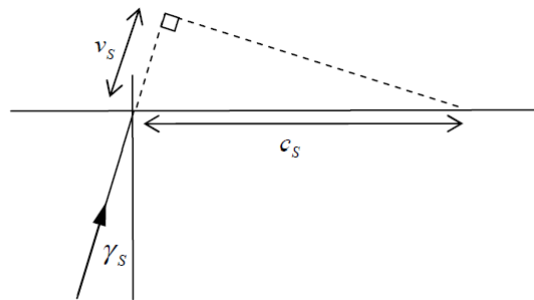


**Figure 4.2.** S-waves apparent propagation velocity (Vertical plane)

When body waves move toward the ground surface, they are refracted toward the normal due to the increasingly softer geological layers. By the time these waves reach the surface, the angle of incidence is generally very small. In practice, body waves arrive almost vertically, resulting in high apparent velocity values relative to the ground surface. The apparent propagation velocity of S-wave is given by –

$$c_s = \frac{v_s}{\sin \gamma_s} \quad (4.8)$$

Where,  $v_s$  = shear wave velocity of surface materials  
 $\gamma_s$  = angle of incidence of S-waves

During the  $M_w$  6.7 Northridge earthquake in 1994, near-field velocity pulses reaching up to 177 cm/s were recorded. O'Rourke et al. (2001) utilized  $v_{ps}$  and  $c_s$  values of 100 cm/s and 2.5 km/s, respectively, to estimate the typical maximum body-wave-induced strains for this event, using Equation (3.5). Despite the high peak ground velocity (PGV), the resulting strain was approximately  $2 \times 10^{-4}$ . Due to the high apparent propagation velocities, the ground strains caused by traveling body waves are usually only significant enough to damage pipelines that are already compromised by corrosion or stress concentrations.

#### 4.1.2. Ground strain caused by surface waves

The most impactful surface-wave movements are generated by Rayleigh waves, which create alternating tensile and compressive strains along the direction of propagation. As R-waves move parallel to the ground surface, their apparent propagation velocity matches the phase velocity,  $c_{ph}$ . The phase velocity is the rate at which a vertical disturbance at a specific frequency, starting at the ground surface, spreads across the surface of the medium (O'Rourke & Liu, 1999).

$$C_{ph} = \lambda f \quad (4.9)$$

Where,  $\lambda$  = wavelength  
 $F$  = frequency

The frequency dependence can be quantified using a dispersion curve. Various researchers have derived these curves for different layered soil profiles. Figure 4.3 illustrates a normalized dispersion curve for a uniform layer of thickness (H), characterized by a shear-wave velocity  $v_{soil}$  (km/s) and Poisson's ratio  $\mu_{soil}$ , overlying a half-space with shear-wave velocity  $v_{Srock}$  (km/s) and Poisson's ratio  $\mu_{rock}$ .

O'Rourke et al. (1984) demonstrated that at low frequencies (below 0.25 times the ratio of the shear wave velocity of the soil to the thickness of the soil layer), the phase velocity ( $c_{ph}$ ) is slightly less than the shear wave velocity of the underlying half-space. This is because the wavelength is much larger than the thickness of the soil layer, making the properties of the overlying soil layer negligible. At high frequencies (greater than 0.5 times the ratio of the shear wave velocity of the soil to the thickness of the soil layer), the wavelength becomes comparable to or smaller than the thickness of the surface layer, causing the phase velocity to be influenced primarily by the properties of the surface layer. For intermediate frequencies, both the properties of the soil layer and the half-space need to be considered. O'Rourke et al. (1984) simplified the relationship between phase velocity and frequency for a single layer

overlying a half-space into a tri-linear relationship, which can be extended to multiple layered soil profiles.

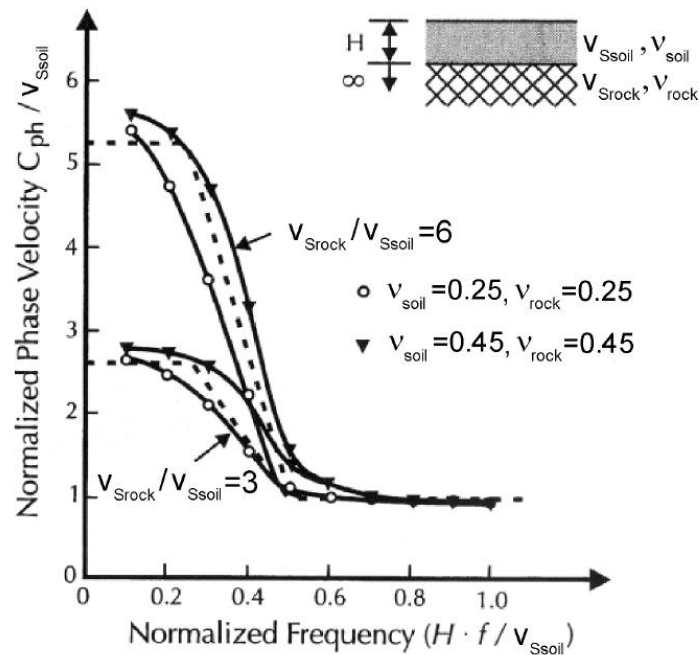


**Figure 4.3.** Normalised dispersion curve for a single layer over a half space (O'Rourke et al., 1984)

## 5.2. Factors influencing the earthquake susceptibility of pipelines

Numerous studies have investigated the factors affecting pipeline vulnerability under non-catastrophic (aseismic) operating conditions. Due to the challenges in characterizing the condition of buried pipelines, many findings have been inconclusive. However, several key factors influencing pipe leakage and break rates (per unit length of pipe) have been identified. In a literature review spanning from 1948 to 1991, Wengstrom (1993) examined the impact of various factors, including pipe age, installation method, material type, pipe dimensions (diameter and thickness), joint type, previous damage history, operating pressure, soil conditions, land use, and seasonal variations of the external environment. Many of these factors are also crucial for understanding pipeline vulnerability under seismic conditions.

**Table 4.2.** Some commonly-used pipeline-related abbreviations, together with typical yield stress and yield strain values for common pipe barrel materials (from O'Rourke & Liu, 1999)

Abbreviation	Term	Typical yield stress $\sigma_y$ (MPa)	Typical yield strain $\epsilon_y$
AC	Asbestos Cement	†	†
C	Concrete	2-28	0.0001-0.0003
CI	Cast Iron	97-290	0.001-0.003
DI	Ductile Iron	290-360	0.0018-0.0022
PE	Polyethylene	15-17	0.022-0.025
PVC	Polyvinyl Chloride	35-45	0.017-0.022
S	Steel	227, 289, 358, 448, 517*	0.00134, 0.00231**
SG	Steel (threaded joint)	-	-
WS	Welded Steel	-	-
WSAWJ (A, B)	Welded Steel arc-welded joints (Grade A & B steel)	-	-
WSAWJ (X)	Welded Steel	-	-
WSCJ	Welded Steel	-	-
WSGW J	Welded Steel	-	-

† AC does not have yield values due to its brittleness. Its strength is normally characterised using transverse crushing strength or beam strength.

\* Values are quoted for five different grades of steel: B, X-42, X-52, X-65 & X-70 respectively.

\*\* Values are given for X-42 and X-65 grades of steel.

Seismic loading can lead to various failure modes in pipelines. For corrosion-free continuous pipelines, such as steel pipes with welded joints, the primary failure modes include rupture due to axial tension, local buckling from axial compression, and flexural failure. At shallow burial depths, these pipelines may also experience beam buckling under compression. For corrosion-free segmented pipelines with bell and spigot joints, the main failure modes are axial pull-out at the joints, joint crushing, and round flexural cracks in pipe segments away from the joints.

O'Rourke & Liu (1999) provide failure criteria for each of these modes. The presence of corrosion in cast iron (CI), ductile iron (DI), or steel pipes increases the likelihood of failure by reducing pipe wall thickness. Corrosion is linked to pipeline age but is significantly influenced by soil conditions, such as pH, soil resistivity, and soil aeration. Asbestos cement (AC) pipes are weakened by lime leaching (decalcification), while PVC pipes are susceptible to fatigue.

The influence of pipe age is also related to environmental changes and evolving practices in pipe installation and material selection. Certain elements of a pipeline network, such as elbows and intersections, are more vulnerable to earthquake damage due to stress concentrations induced by seismic waves. Stresses at these points can significantly exceed those in adjacent straight pipe sections (Stuart et al., 1996; Datta, 1999). Additionally, pipes connecting to manholes, tanks, or buildings are prone to differential movements, increasing their vulnerability.

## CHAPTER 5

# GUWAHATI CASE STUDY: CHARACTERISTICS AND EFFECTS

---

The 1950 Assam earthquake, one of the most significant seismic events in the 20th century, profoundly affected the region, including Guwahati. The earthquake, with a magnitude of Mw 8.7, occurred in a tectonically active area dominated by the collision of the Indian Plate with the Eurasian Plate. This tectonic setting is characterized by complex fault systems, including the Oldham Fault and the Kopili Fault, which have historically generated powerful earthquakes.

The North-East Indian region, including Assam, is situated at the northeastern boundary of the Indian Plate, which is being subducted beneath the Eurasian Plate. This tectonic interaction results in significant seismic activity, with the Indian Plate moving northwards at a rate of approximately 50 mm per year. The 1950 Assam earthquake was a result of this tectonic collision, causing extensive ground deformation, landslides, and soil liquefaction.

### 5.1. Tectonic Setting and Fault Systems

The tectonic setting of the area covered by the 1950 Assam earthquake is illustrated in Figure 6.1. The earthquake occurred in a region dominated by the complex interaction of the Indian and Eurasian Plates. The Oldham Fault, located to the west of Guwahati, and the Kopili Fault, to the east, are significant fault systems in this region. These faults form the boundaries of the tectonic plates and are responsible for the seismic activity in Assam.

The Oldham Fault is a right-lateral strike-slip fault, extending over 1000 km from the eastern Himalayas to the Shillong Plateau. The fault forms the northern boundary of the Indian Plate, which is being squeezed northwards by the collision with the Eurasian Plate. GPS measurements have shown this motion to be at the rate of about 50 mm per year (Jackson, 2001).

A detailed fault map for the whole of Assam has been compiled by the Geological Survey of India (GSI) (Saroglu et al., 1992). The structure and kinematics of the Oldham Fault zone in the vicinity of Guwahati have been described in detail by Neugebauer (1995). The fault passes approximately 30 km to the west of Guwahati, near the Brahmaputra River. In this locality, the fault branches into two, with the main strand extending to the northwest towards the Shillong Plateau and then westwards to the eastern Himalayas. The southern branch passes

near the Meghalaya Plateau and to the south of the Brahmaputra River, also meeting the eastern Himalayas in the west. The area experiences significant seismic activity characterized mainly by:

- i. Reverse (Thrust) Faulting: This type of faulting is prevalent in Assam due to the ongoing collision between the Indian plate and the Eurasian plate. The Shillong Plateau and the Himalayan Frontal Thrust are key areas where reverse faulting is common. The 1950 Assam earthquake, one of the most significant earthquakes in the region, was associated with thrust faulting.
- ii. Strike-Slip Faulting: Although less common than reverse faulting, strike-slip faulting also occurs in the region. The complex tectonic interactions sometimes result in lateral movements, contributing to strike-slip faulting.
- iii. Normal Faulting: This type of faulting is relatively rare in Assam compared to reverse and strike-slip faulting. The regional tectonic compressive forces are not conducive to normal faulting, which typically occurs in extensional tectonic settings.

Therefore, reverse (thrust) faulting is the most predominant type of faulting in Assam due to the compressional tectonic regime imposed by the Indian-Eurasian plate collision.

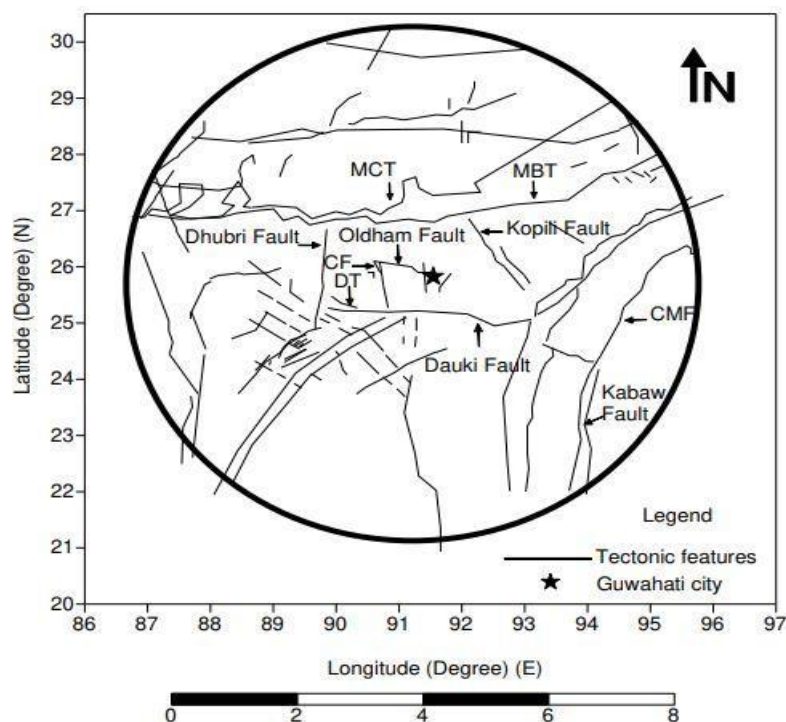


**Figure 5.1.** A map indicating the faults within a 500km radius of Guwahati city, including the Chedrang fault (CF), Churachandpur–Mao fault (CMF), and Dapsi thrust (DT).

## **5.2. Impact on Guwahati**

The 1950 Assam earthquake caused widespread devastation in the region, including significant damage to infrastructure in Guwahati. The earthquake resulted in extensive ground deformation, including fissures and sand vents, which likely affected buried pipelines. The region experienced severe flooding due to landslides damming tributaries of the Brahmaputra River, further complicating the impact on pipeline infrastructure.

In Guwahati, the earthquake's intensity and ground shaking led to significant soil liquefaction, landslides, and ground settlements. The soil profile in Guwahati generally consists of alluvial deposits, with sand, silty sand, silt, and clay layers. The soil strata up to 15 meters depth showed low SPT N-values ranging between 20 and 30, indicating a high susceptibility to liquefaction. The water table in the region typically lies about 2 meters below the surface, although in some locations, it is found at greater depths, up to 15 meters (Basu et al., 2019).

The dynamic site response analysis for Guwahati, considering a uniform depth of 20 meters of soil overlying an elastic bedrock, revealed that the fundamental frequency of the soil layer, considering soil uncertainty, lies in the range of 2.1 to 4.1 Hz. This analysis, conducted by Kumar and Krishna (2013), highlighted the significant influence of soil column depth on the response of soil amplification studies.

The presence of corrosion in cast iron (CI), ductile iron (DI), or steel pipes increased the likelihood of failure by reducing pipe wall thickness. Corrosion is linked to pipeline age but is significantly influenced by soil conditions, such as pH, soil resistivity, and soil aeration. Asbestos cement (AC) pipes were weakened by lime leaching (decalcification), while PVC pipes were susceptible to fatigue. The influence of pipe age is also related to environmental changes and evolving practices in pipe installation and material selection.

Certain elements of the pipeline network in Guwahati, such as elbows and intersections, were more vulnerable to earthquake damage due to stress concentrations induced by seismic waves. Stresses at these points significantly exceeded those in adjacent straight pipe sections (Stuart et al., 1996; Datta, 1999). Additionally, pipes connecting to manholes, tanks, or buildings were prone to differential movements, increasing their vulnerability.

### 5.3. Subsoil data of Guwahati

Most of the data collected for the study region is based on standard penetration tests (SPT). The depth of the soil profile generally varies from 15 to 30 meters, but in some cases, it is less than 15 meters. The soil layer below the surface predominantly consists of sand, silty sand, silt, and clay. The soil strata mainly comprise alluvial soil up to 15 meters depth, with SPT N-values ranging between 20 and 30 (Bandyopadhyay et al., 2022). Kanth et al. (2008) determined the average N-value for 100 sites in the Guwahati region and inferred that most sites fall into Class E according to the Uniform Building Code (1997). The water table in the region typically lies about 2 meters below the surface, although in some locations, it is found at greater depths, up to 15 meters (Basu et al., 2019). Kumar and Krishna (2013) collected N-value profiles for five different sites. Due to the lack of shear wave velocity data at some depths, N-values were converted into shear wave velocities using a correlation function developed for similar site conditions.

The shear wave velocity ( $V_s$ ) profile obtained from this correlation is shown in Figure 5.2, indicating a gradual increase in  $V_s$  with depth. The soil column depth significantly influences the response in soil amplification studies. Kumar and Krishna (2013) conducted a soil amplification study considering a uniform depth of 15.5 meters in all boreholes overlying an elastic bedrock. Bandyopadhyay et al., (2022), a similar methodology is adopted, assuming a 20-meter soil layer overlying an elastic bedrock. In dynamic site response analysis, the shear modulus ( $G$ ) of the soil is required, which is obtained from shear wave velocity using Eq. (11). Three different shear moduli,  $0.5G$ ,  $G$ , and  $2G$ , are used in the analysis (Bandyopadhyay et al., 2021b) to account for uncertainty in soil parameters. The fundamental frequency of the soil layer, considering soil uncertainty, ranges from 2.1 to 4.1 Hz.

**Table 5.1.** PGA and  $S_a/g$  at 0.1 s values of six cities in Assam state (Bandyopadhyay et al., 2022)

City	PGA (g)				S1/g (T=0.1 s, 5% damping)			
	RP 475	RP 975	RP 2475	RP 9975	RP 475	RP 975	RP 2475	RP 9975
<b>Jorhat</b>	0.22	0.28	0.38	0.54	0.55	0.7	0.92	1.33
<b>Dibrugarh</b>	0.22	0.28	0.37	0.53	0.53	0.68	0.9	1.27
<b>Silchar</b>	0.24	0.34	0.5	0.8	0.54	0.92	1.4	2.1
<b>Tezpur</b>	0.25	0.32	0.42	0.63	0.55	0.71	1	1.38
<b>Guwahati</b>	0.24	0.32	0.42	0.63	0.57	0.74	1	1.32
<b>Nagaon</b>	0.22	0.28	0.37	0.55	0.53	0.68	0.9	1.32

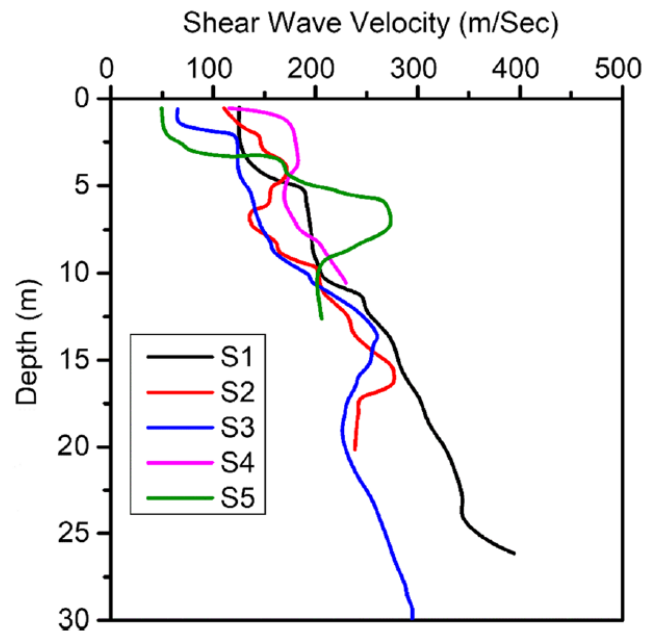


**Figure 5.2.** Shear wave velocity profile of the five different locations of Guwahati city (Bandyopadhyay et al., 2022)

#### 5.4. Design Calculation

The design of this continuous pipeline is based on the IITK-GSDMA guidelines and has been checked for the four cases mentioned in the guidelines: Permanent Ground Displacement (PGD), Buoyancy due to Liquefaction, Fault Crossing, and Seismic Wave Propagation. All the data used in this study are specific to Guwahati, derived from an extensive literature review. Standard pipeline details have been considered in the design.

## CALCULATION FOR OPERATIONAL STRAIN IN THE PIPELINE

### Given Data:

Pipe Grade = **X-52** (Table 3.7.4)

For the above grade of pipe, Yield stress of pipe material

$\sigma_y$	=	<b>358</b>	Mpa
Rameberg-Osgood parameter ( <b>n</b> )	=	9	
Rameberg-Osgood parameter ( <b>r</b> )	=	10	

Pressure (carried by pipeline)	=	3	MPa
Installation Temperature	=	30	°C
Operating Temperature	=	35	°C
Outer Diameter of pipe (D)	=	0.6	m
Thickness of pipe (t)	=	0.0064	m
Poisson's ratio ( $\mu$ )	=	0.3	(Generally 0.3 for steel)
Coefficient of thermal expansion	=	0.000012	
Young's modulus of elasticity	=	2E+11	N/m <sup>2</sup>

### For a continuous pipeline

#### a) Pipe strain due to internal pressure

Longitudinal stress in pipe,

$$S_p = P \times D \times \mu / 2 t = \mathbf{42.19} \text{ MPa}$$

Longitudinal strain in pipe,

$$\epsilon_p = S_p (1 + (n / 1+r) (S_p / \sigma_y)^r) / E = \mathbf{0.021\%} \text{ (tensile)}$$

#### a) Pipe strain due to temperature change

Longitudinal stress in pipe,

$$S_T = E \times \alpha \times (T_2 - T_1) = \mathbf{12000000} \text{ N/m}^2$$

$$= \mathbf{12} \text{ MPa}$$

Longitudinal strain in pipe,

$$\epsilon_t = S_t (1 + (n / 1+r) (S_t / \sigma_y)^r) / E = \mathbf{0.006\%} \text{ (tensile)}$$

So, the total strain in continuous pipeline due to internal pressure and temperature

$$= 0.021\% + 0.006\% = 0.03\%$$

Operational strain in pipe ( $\epsilon_{oper}$ ) = **0.03%**

<b>Calculation of Soil Spring</b>				
Soil cover (H)	=	1.2	m	
Cohesion (c)	=	30	kPa	
Angle of friction ( $\phi$ )	=	30	°	
Eff. Unit weight ( $\gamma'$ )	=	18	kN/m <sup>3</sup>	
Pipe Coating	=	<b>Smooth steel</b>		(Table B 1a)
<b>(a) Axial Soil spring</b>				
Max. soil resistance per unit length of pipe (Annex-B)				
$t_u$	=	$(\pi \times D \times c \times \alpha) + (\pi \times D \times H \times \gamma') \times ((1 + K_o) / 2) \times \tan \delta'$		
	=	<b>67916</b>	N/m	= <b>67.9</b> kN/m
$\alpha$	=	0.9965		
Interface angle of friction b/w soil & pipe				
$\delta'$	=	$f \times \phi$	=	<b>0.7</b> x 30
			=	21 °
Coefficient of soil pressure at rest				
$K_o$	=	$1 - \sin \phi$	=	0.48
Mobilizing soil displacement in <b>Axial direction</b>				
	=	$\Delta_t$		
	=	<b>0.005</b> m		
<b>(b) Lateral Soil spring</b>				
Max. transverse soil resistance per unit length of pipe				
$P_u$	=	$N_{ch} \times c \times D + N_{qh} \times \gamma' \times H \times D$		
	=	<b>193454</b>	N/m	= <b>193.5</b> kN/m
x	=	H / D	=	2
a	=	4.565		
b	=	1.234		
c	=	-0.089		
d	=	4.27E-03		
e	=	-9.16E-05		(Table B2)
$N_{ch}$	=	$a + (bx) + (c / (x+1)^2) + (d / (x+1)^3) \leq 9$		
	=	5.916		(For sandy soil = 0)
$N_{qh}$	=	$a + bx + cx^2 + dx^3 + ex^4$		
	=	6.7097		

The mobilizing displacement of soil in <b>Lateral direction</b>						
$\Delta_p$	=	$0.04 (H + D / 2)$	=	<b>0.06</b>	m	
<b>(c) Vertical Soil spring</b>						
<b>Uplift :</b>						
Max. uplift soil resistance per unit length of pipes						
$Q_u$	=	$N_{cv} \times c \times D + N_{qv} \times \gamma' \times H \times D$				
	=	89677	N/m	=	<b>89.7</b>	kN/m
$N_{cv}$	=	$2 (H / D)$	$\leq$	10	=	4
$N_{qv}$	=	$\phi \times H / 44 \times D$	$\leq$	$N_q$		
	=	1.364				
Mobilizing displacement of soil in vertical uplift						
$\Delta_{qu}$	=	$0.15 \times H$	=	<b>0.18</b>	m	
<b>Bearing :</b>						
Max. bearing soil resistance per unit length of pipes						
$Q_d$	=	$N_c \times c \times D + N_q \times \gamma' \times H \times D + N_v \times \gamma \times D^2 / 2$				
	=	831600	N/m	=	<b>831.6</b>	kN/m
$N_c$	=	30				
$N_q$	=	18	(From figure B 3b)			
$N_v$	=	18				
Mobilizing displacement of soil in vertical bearing						
$\Delta_{qd}$	=	$0.125 \times D$	=	<b>0.075</b>	m	
<b>Summary of Result</b>						
Soil Site	Direction of pipe movement		Max. soil resistance (kN/m)		Mobilizing soil displacement (m)	
Guwahati	Axial		$t_u$	67.9	$\Delta_t$	0.005
	Lateral		$P_u$	193.5	$\Delta_p$	0.06
	Vertical	Uplift	$Q_u$	89.7	$\Delta_{qu}$	0.18
	Vertical	Bearing	$Q_d$	831.6	$\Delta_{qd}$	0.075

## EVALUATION OF SEISMIC SAFETY OF CONTINUOUS PIPELINE

### Given data:

Pressure in pipeline (P)	=	3	MPa
Class of Pipeline	=	I	(Table 3.5.2)
Earthquake condition	=	Transverse & Longitudinal PGD	
Installation Temperature	=	30	°C
Operating Temperature	=	35	°C
Pipe grade	=	X-52	
Diameter of pipe (D)	=	0.6	m
Thickness of pipe (t)	=	0.0064	m
Operational strain in pipeline	=	0.03%	

### Case 1: Permanent Ground Displacement (PGD)

#### (i) Parallel crossing (Longitudinal PGD)

Length of PGD zone	=	100	m
Width of PGD zone	=	40	m
Ground displacement due to liquefaction ( $\delta^l$ )	=	2	m
Design ground movement			
$\delta^l_{design}$	=	$\delta^l$	x $I_p$ (Table 3.5.2)
	=	2	x 1.5
	=	3.00	m

(i) The amount of ground movement ( $\delta^l_{design}$ ) is considered to be large and the pipe strain is controlled by length (L) of PGD zone

Peak pipe strain :

$$\epsilon_a = (t_u L / 2 \pi D t E) \times [1 + (n / 1+r) (t_u L / 2 \pi D T \sigma_v)^r]$$

$$= \mathbf{0.00151}$$

(ii) The length (L) of PGD zone is large, and the pipe strain is controlled by amount of ground movement ( $\delta^l_{design}$ )

Peak pipe strain :

$$\epsilon_a = (t_u L_e / 2 \pi D t E) \times [1 + (n / 1+r) (t_u L_e / 2 \pi D T \sigma_v)^r]$$

$$= \mathbf{0.08518}$$

$$L_e = 183.496103$$

(Effective length of pipeline over which the friction force ( $t_u$ ) acts)

Design strain in pipe [least value between two cases (i) & (ii)]

$$\epsilon_{seismic} = \mathbf{0.00151}$$

Operational strain in pipe ( $\epsilon_{oper}$ )	=	0.03%			
Hence,					
<b>Total Tensile strain in pipeline</b>	=	0.151%	+	0.03%	
	=	<b>0.00178</b>			
<b>Total Compressive strain in pipeline</b>	=	0.151%	-	0.03%	
	=	<b>0.00124</b>			
Pipe Component	=	<b>Steel pipe</b>		(Table 3.9.1)	
<b>Limiting strain in tension for PGD</b>	=	<b>0.03</b>			
Total strain in pipe due to longitudinal strain is less than allowable strain					
	=	<b>SAFE</b>			
<b>(i) Transverse crossing (Transverse PGD)</b>					
Ground displacement due to liquefaction ( $\delta^l$ )	=	2	m		
Design transverse ground displacement ( $\delta^t_{design}$ )					
$\delta^t_{design}$	=	$\delta^t$	x	$l_p$	
	=	2	x	1.5	
	=	3	m		
Max. bending strain in the pipe					
a)	$\epsilon_b$	=	$\mp (\pi D \delta^t_{design}) / W^2$		
		=	$\mp$	0.00353	
b)	$\epsilon_b$	=	$\mp (P_u W^2 / 3 \pi E t D^2)$		
		=	$\mp$	0.0713	
Hence,					
Max. strain induced in the pipeline due to transverse PGD					
	=	$\epsilon_{seismic}$			
	=	$\mp$	0.0035	(tensile / compressive)	
<b>Total longitudinal strain in pipe in tension</b>					
	=	0.0035343	+	0.0003	
	=	<b>0.0038</b>			
<b>Total longitudinal strain in pipe in compression</b>					
	=	0.0035343	-	0.0003	
	=	<b>0.0033</b>			
<b>Allowable strain in tension for PGD</b>					
	=	<b>0.03</b>			
<b>Allowable strain in compression for steel pipe</b>					
	=	$\epsilon_{cr-c}$			
	=	0.175 x t / R			
	=	$\epsilon_{cr-c}$	=	0.0037333	
Total strain in pipe due to transverse PGD is less than allowable strain for tension					
	=	<b>SAFE</b>			
Total strain in pipe due to transverse PGD is less than allowable strain for compression					
	=	<b>SAFE</b>			

<b>Case 2: Buoyancy due to Liquefaction</b>					
<b>Given data:</b>					
Extent of liquefaction ( $L_b$ )	=	40	m		
Unit weight of saturated soil at site	=	18	$\text{kN/m}^3$		
Unit weight of fluid	=	10	$\text{kN/m}^3$		
Unit weight of pipe	=	78.56	$\text{kN/m}^3$		
Net upward force per unit length of pipeline					
$F_b$	=	$\pi D^2 / 4 \times (Y_{\text{sat}} - Y_{\text{content}}) - \pi D t \gamma_{\text{pipe}}$			
	=	1314	N/m		
Bending force in pipeline due to uplift force ( $F_b$ )					
$\sigma_{\text{bf}}$	=	$\mp F_b L_b^2 / 10 Z$			
	=	$\mp 1.2\text{E}+08$	$\text{N/m}^2$		
(Z : section modulus)	Z	=	0.001752471	$\text{m}^4$	
Max. strain in 7pipe corresponding to above bending stress					
$\epsilon$	=	$(\sigma_{\text{bf}} / E) [1 + (n / 1 + r) (\sigma_{\text{bf}} / \sigma_y)^r]$			
	=	0.0006	(tensile / compressive)		
Hence,					
<b>Total longitudinal strain in pipe in tension</b>	=	0.0006	+	0.0003	
	=	<b>0.0009</b>			
<b>Total longitudinal strain in pipe in compression</b>	=	0.0006	-	0.0003	
	=	<b>0.0003</b>			
<b>Allowable strain in pipe in tension</b>	=	<b>0.03</b>			
<b>Allowable strain in pipe in compression</b>	=	$\epsilon_{\text{cr-c}}$			
	=	$0.175 \times t / R$			
	=	<b>0.00373</b>			
The maximum strain in pipeline due to buoyancy effect is less than the allowable strain in tension					
	=	<b>SAFE</b>			
The maximum strain in pipeline due to buoyancy effect is less than the allowable strain in compression					
	=	<b>SAFE</b>			

<b>Case 3: Fault Crossing</b>					
<b>Given data:</b>					
Type of Fault displacement	=	<b>Reverse</b>	(Clause 6.1..1)		
Magnitude of earthquake	=	<b>7.1</b>			
Expected normal-slip fault displacement	=	$\delta_{fn}$	=	0.842	m
Dip angle of fault movement	=	$\psi$	=	35	°
Angle b/w pipeline & fault line	=	$\beta$	=	40	°
Source to site distance	=		=	20	km
Component of fault displacement in axial direction of pipeline					
$\delta_{fax}$	=	$\delta_{fn} \cos\psi \sin\beta$			
	=	0.443	m		
Component of fault displacement in transverse direction of pipeline					
$\delta_{ftr}$	=	$\delta_{fn} \cos\psi \cos\beta$			
	=	0.528	m		
Importance factor ( $I_p$ )	=	2.3			
Design fault displacement in axial direction					
	=	$\delta_{fax-design}$			
	=	$\delta_{fax}$	x	$I_p$	
	=	0.443	x	2.3	
	=	1.02	m		
Design fault displacement in transverse direction					
	=	$\delta_{ftr-design}$			
	=	$\delta_{ftr}$	x	$I_p$	
	=	0.528	x	2.3	
	=	1.22	m		
Average pipe strain due to fault movement in axial direction					
$\epsilon$	=	$2 [ (\delta_{fax-design} / 2 L_a) + (\delta_{ftr-design} / 2 L_a)^2 / 2 ]$			
	=	0.014	(tensile)		
$L_a$	=	$E_i \epsilon_y \pi D t / t_u$	=	71.05	m
Or,					
$L_a$	=	100	m (Actual length of anchorage)		
Hence, anchored length to be considered					
	=	71.05	m		
<b>Total strain in pipe in tension</b>					
	=	0.014	+	0.0003	
	=	<b>0.015</b>			
<b>Allowable strain in pipe in tension</b>					
	=	<b>0.03</b>			
The total tensile strain in pipeline due to fault crossing is less than the allowable strain in tension					
	=	<b>SAFE</b>			



## **5.5. Parametric Study**

A comprehensive parametric analysis is conducted to evaluate the strain variations in buried water pipelines with different pipe diameters and wall thicknesses under seismic loading conditions. The pipe diameters considered in the analysis were 0.2 m, 0.4 m, 0.6 m, and 0.8 m, while the pipe thicknesses ranged from 0.004 m to 0.012 m, increasing in increments of 0.001 m. The analysis aimed to understand the influence of these parameters on the overall strain experienced by the pipelines.

The strains considered for the parametric studies are as follows:

- Strain due to PGD
- Buoyancy due to Liquefaction
- Fault Crossing
- Seismic Wave Propagation

This strain was calculated based on the IITK-GSDMA guidelines, ensuring a comprehensive assessment of the pipeline's performance under various seismic scenarios. The results of the strain vs. pipe thickness variation are presented in the following sections, highlighting the critical role of pipe thickness in mitigating seismic-induced strains.

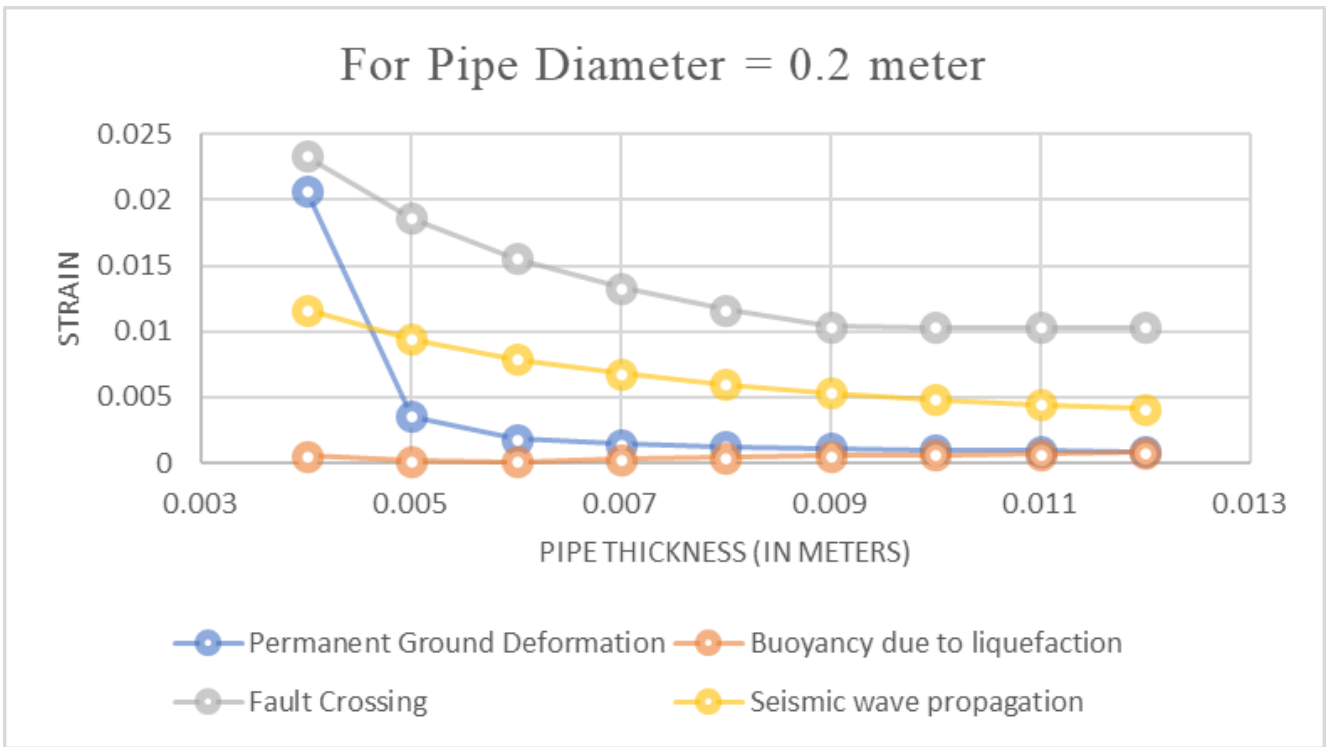


**Figure 5.3.** Strain Vs Pipe thickness for pipe diameter 0.2 m

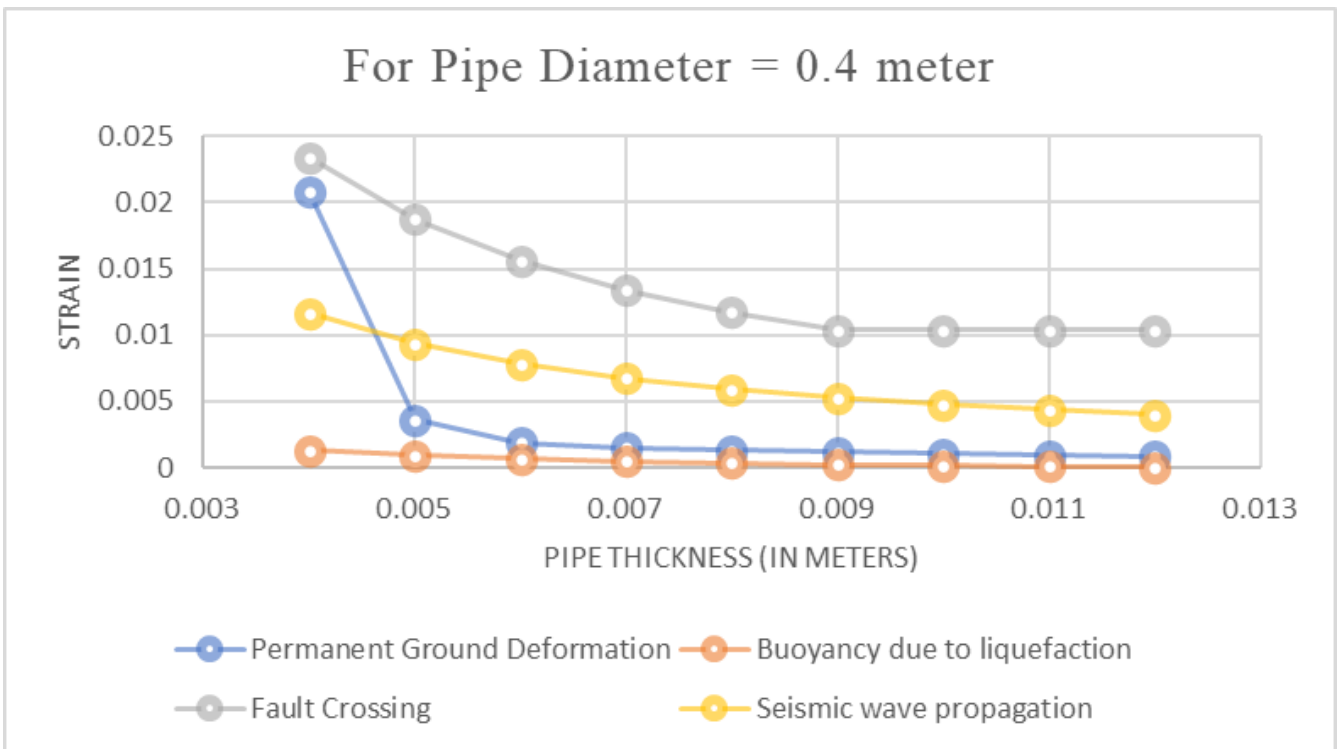


**Figure 5.4.** Strain Vs Pipe thickness for pipe diameter 0.4 m

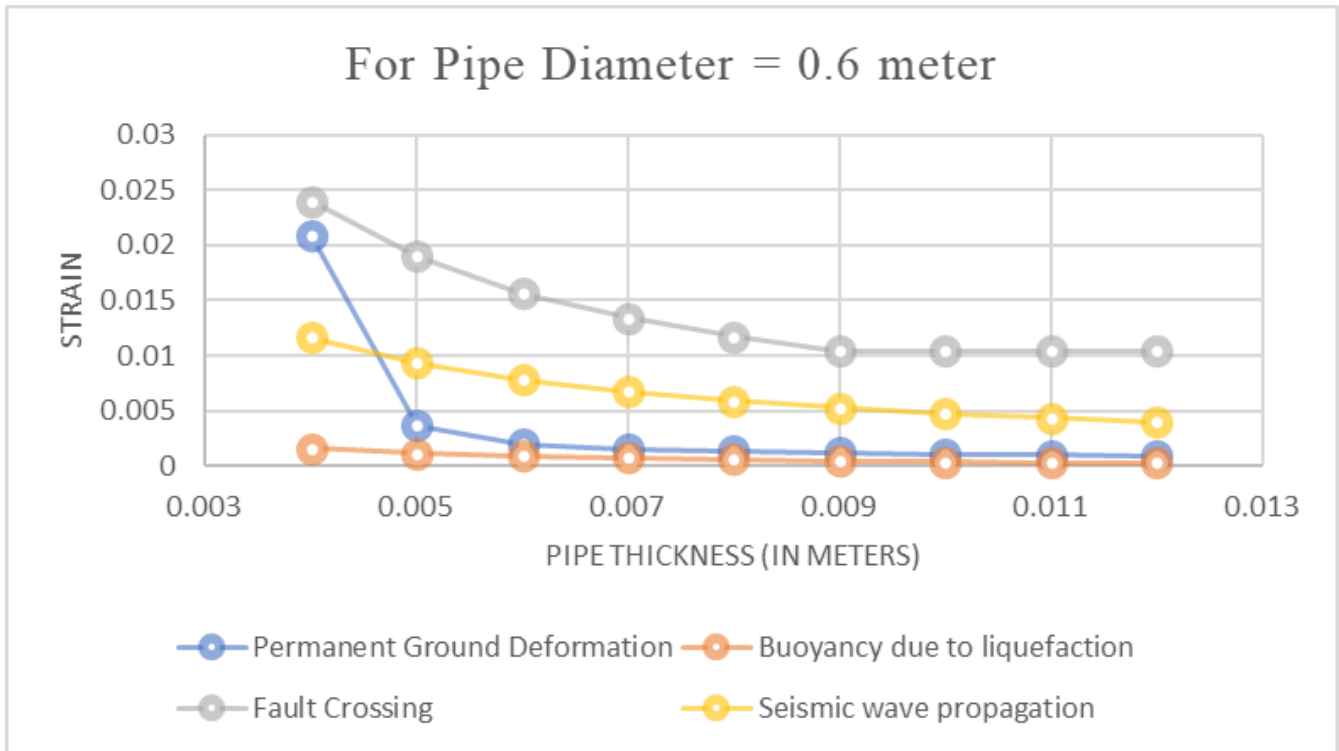


**Figure 5.5.** Strain Vs Pipe thickness for pipe diameter 0.6 m

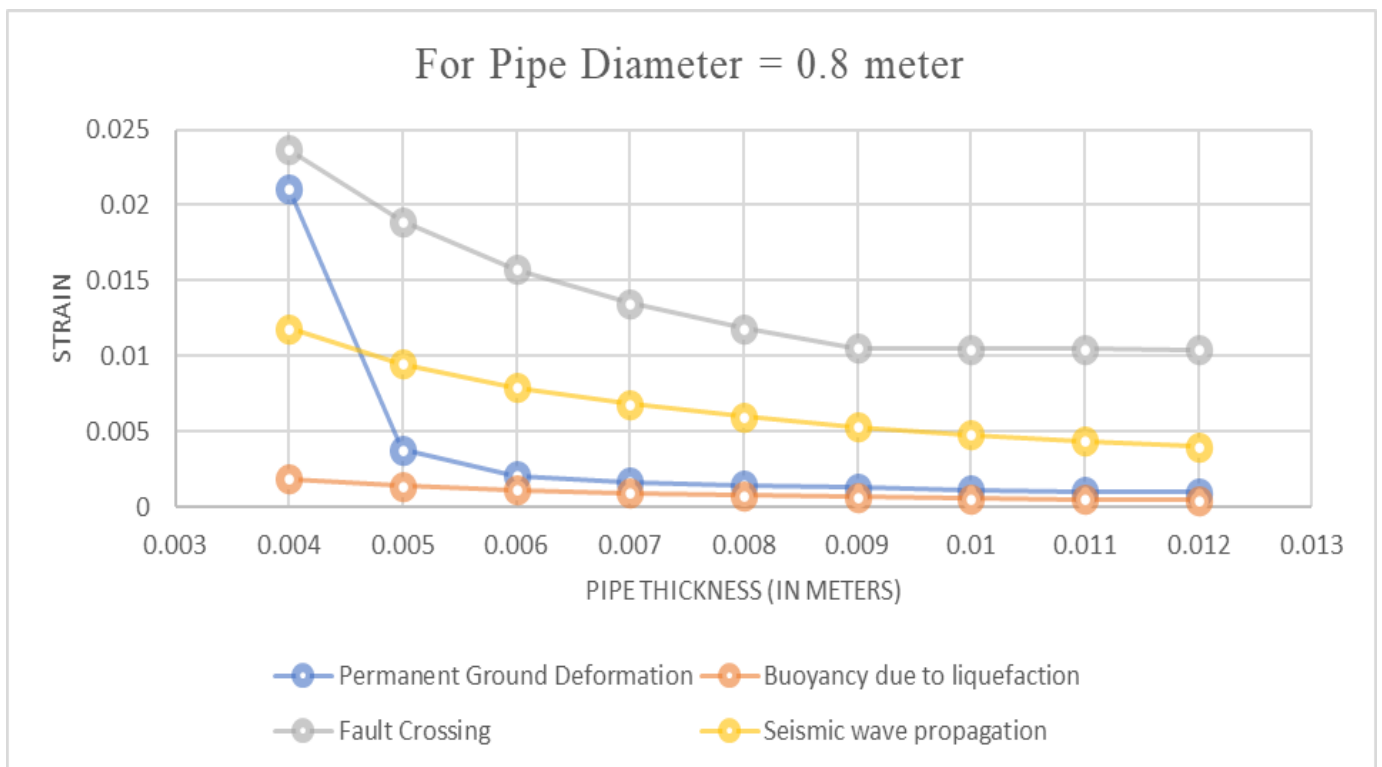


**Figure 5.6.** Strain Vs Pipe thickness for pipe diameter 0.8 m

# DISCUSSION ON RESULTS

---

The parametric study conducted in this research aimed to evaluate the strain variations in buried water pipelines with different pipe diameters and wall thicknesses under seismic loading conditions. The analysis considered pipe diameters of 0.2 m, 0.4 m, 0.6 m, and 0.8 m, with thicknesses ranging from 0.004 m to 0.012 m, increasing in increments of 0.001 m.

### 6.1. Key Observations

#### 1. Strain vs. Pipe Thickness for Diameter 0.6 m

As the pipe thickness increases from 0.004 m to 0.012 m, the total axial strain decreases significantly. For a pipe thickness of 0.004 m, the total axial strain is 0.0117, while for a thickness of 0.012 m, it reduces to 0.004002. This indicates that increasing the pipe thickness enhances the pipeline's resistance to seismic-induced strains.

#### 2. Strain vs. Pipe Thickness for Diameter 0.4 m

Similar to the 0.6 m diameter, increasing the pipe thickness from 0.004 m to 0.012 m results in a decrease in total axial strain. The total axial strain decreases from 0.011658 for a thickness of 0.004 m to 0.004004 for a thickness of 0.012 m. This trend demonstrates the importance of pipe thickness in mitigating seismic-induced strains.

#### 3. Strain vs. Pipe Thickness for Diameter 0.2 m

For the smallest diameter considered (0.2 m), the total axial strain also decreases with increasing pipe thickness. The total axial strain reduces from 0.011662 for a thickness of 0.004 m to 0.00409 for a thickness of 0.012 m. This further confirms the positive impact of increased pipe thickness on strain reduction.

#### 4. Strain vs. Pipe Thickness for Diameter 0.8 m

For the largest diameter considered (0.8 m), the total axial strain follows the same decreasing trend with increasing pipe thickness. The total axial strain decreases from 0.011826 for a thickness of 0.004 m to 0.00402 for a thickness of 0.012 m. This consistency across different diameters highlights the general effectiveness of increasing pipe thickness in reducing seismic-induced strains.

The results of the parametric study clearly indicate that increasing the pipe thickness significantly reduces the total axial strain experienced by the pipelines under seismic loading conditions. This trend is consistent across all pipe diameters considered in the study (0.2 m, 0.4 m, 0.6 m, and 0.8 m). The reduction in strain with increased thickness can be attributed to the enhanced structural integrity and resistance to deformation provided by thicker pipes.

The study also highlights the importance of considering multiple factors (seismic wave propagation, soil friction, and operational conditions) in the assessment of pipeline performance. The combined strain (Strain 4) provides a comprehensive measure of the pipeline's response to seismic loading, ensuring a holistic evaluation of its seismic resilience.

The findings from this parametric study underscore the critical role of pipe thickness in the design of buried pipelines in earthquake-prone regions. By optimizing the pipe thickness, it is possible to enhance the seismic resilience of the pipeline network, thereby reducing the risk of failure during seismic events.

## **GEOPHYSICAL INVESTIGATION**

---

### **7.1. Electrical Resistivity Tomography (ERT)**

Electrical Resistivity Tomography (ERT) is a geophysical method used to image subsurface structures by measuring the electrical resistivity of the ground. This technique is particularly useful for mapping variations in soil and rock properties, such as moisture content, porosity, and mineral composition. ERT is effective in detecting voids, cavities, and changes in material properties, making it valuable for pipeline inspection.

#### **7.1.1 Methodology**

ERT involves placing electrodes in the ground along a survey line. A known electrical current is injected into the ground through a pair of current electrodes, and the resulting potential difference is measured between pairs of potential electrodes. This process is repeated with different electrode pairs to collect a comprehensive dataset. The collected data is then processed using inversion algorithms to create a resistivity model of the subsurface, which is interpreted to identify subsurface features such as lithology, water content, and voids.

#### **7.1.2 Advantages**

- i. High Resolution: Provides detailed images of subsurface structures.
- ii. Cost-Effective: Suitable for various applications like geothermal reservoir identification.
- iii. Versatile: Can be used in 2D, 3D, and 4D imaging.
- iv. Sensitive to Water Content: Useful in detecting variations in water saturation and lithology.

#### **7.1.3 Disadvantages**

- i. Limited Depth Penetration: Depth of investigation is limited by electrode spacing.
- ii. Non-Trivial Modeling: Requires complex data interpretation and modeling.
- iii. Geological Overlap: Can be affected by overlapping geological features.

#### **7.1.4 Application for Pipeline Maintenance**

ERT can be used to detect areas of potential corrosion, voids, or changes in soil properties around pipelines. This is particularly useful for identifying areas where the pipeline may be at risk due to subsidence or other ground movements. After a catastrophic event, ERT

can help assess the integrity of the pipeline by identifying any changes in the surrounding soil that could indicate damage.

## **7.2. Ground Penetrating Radar (GPR)**

Ground Penetrating Radar (GPR) is a non-invasive geophysical method that uses radar pulses to image the subsurface. It is effective in detecting buried objects, changes in material properties, and voids. GPR is particularly useful for shallow subsurface investigations.

### **7.2.1 Methodology**

GPR involves a transmitter and receiver antenna that are moved along the ground surface. The transmitter emits high-frequency electromagnetic pulses into the ground, which reflect off subsurface structures and return to the receiver. The receiver records the reflected signals, creating a profile of the subsurface. The collected data is processed to create images of the subsurface structures, which are interpreted to identify features such as buried objects, voids, and changes in material properties.

### **7.2.2 Advantages**

- i. Non-Destructive: Does not disturb the subsurface.
- ii. Real-Time Data: Provides immediate results.
- iii. Versatile: Effective across various materials like soil, rock, and concrete.
- iv. High Resolution: Offers detailed images of subsurface features.

### **7.2.3 Disadvantages**

- i. Depth Restrictions: Limited penetration depth, especially in high-conductivity materials like clay.
- ii. Complex Interpretation: Requires significant training to interpret data accurately.
- iii. Affected by Moisture: Performance can be impacted by moisture content in the ground.

### **7.2.4 Application for Pipeline Maintenance**

GPR is highly effective in detecting shallow subsurface anomalies such as voids, cracks, or changes in material properties around pipelines. This makes it useful for routine inspections and for assessing damage after events like earthquakes or landslides. GPR can quickly identify areas that need further investigation or immediate repair.

### **7.3. Seismic Surface Refraction Tomography (SSRT)**

Seismic Surface Refraction Tomography (SSRT) is a method that uses seismic waves to map subsurface structures. It is particularly useful for identifying layered structures and changes in material properties. SSRT is effective for shallow investigations.

#### **7.3.1 Methodology**

SSRT involves placing geophones along a survey line at regular intervals. A seismic source (e.g., hammer, explosives) generates seismic waves at the surface, which travel through the subsurface and refract at layer boundaries. The refracted waves are recorded by the geophones, and the travel times are used to create a velocity model of the subsurface. The velocity model is interpreted to identify different geological layers and structures.

#### **7.3.2 Advantages**

- i. • Detailed Subsurface Imaging: Provides information on subsurface velocity structures.
- ii. • Non-Invasive: Does not require drilling or excavation.
- iii. • Effective for Layered Structures: Useful in identifying horizontal and gently dipping layers.

#### **7.3.3 Disadvantages**

- i. • Limited to Shallow Depths: Effective only for relatively shallow investigations.
- ii. • Complex Data Processing: Requires sophisticated algorithms for data interpretation.
- iii. • Sensitive to Noise: Can be affected by surface noise and environmental conditions.

#### **7.3.4 Application for Pipeline Maintenance**

SSRT can be used to map the subsurface layers and identify areas of potential instability around pipelines. This is particularly useful in areas prone to landslides or subsidence. After a catastrophic event, SSRT can help assess the extent of ground movement and its impact on the pipeline.

### **7.4. Crosshole Seismic Tomography (CST)**

Crosshole Seismic Tomography (CST) involves placing seismic sources and receivers in boreholes to create detailed images of the subsurface. It is useful for high-resolution imaging of specific areas.

#### **7.4.1 Methodology**

CST involves placing seismic sources and receivers in boreholes. Seismic waves are generated in one borehole and travel through the subsurface to be recorded in another borehole. The travel times of the seismic waves are recorded and used to create a detailed velocity model of the area between the boreholes. The velocity model is interpreted to identify subsurface structures and material properties.

#### **7.4.2 Advantages**

- i. High Resolution: Provides detailed images of subsurface structures.
- ii. Accurate Velocity Measurements: Useful for determining seismic velocities and material properties.
- iii. Effective for Small Areas: Ideal for detailed investigations of specific zones.

#### **7.4.3 Disadvantages**

- i. Expensive: Requires drilling multiple boreholes.
- ii. Time-Consuming: Data acquisition and processing can be slow.
- iii. Limited Coverage: Effective only for the area between the boreholes.

#### **Application for Pipeline Maintenance**

CST is useful for detailed investigations of specific areas where the pipeline may be at risk. It can provide high-resolution images of the subsurface, identifying potential voids, fractures, or changes in material properties that could impact the pipeline. After a catastrophic event, CST can help assess the extent of damage and guide repair efforts.

### **7.5. Crosshole Seismic Profiling (CSP)**

Crosshole Seismic Profiling (CSP) involves placing seismic sources and receivers in boreholes to measure the travel times of seismic waves. This data is used to create profiles of seismic velocities, which can be interpreted to identify subsurface structures.

#### **7.5.1 Methodology**

CSP involves placing seismic sources and receivers in boreholes. Seismic waves are generated in one borehole and travel through the subsurface to be recorded in another borehole. The travel times of the seismic waves are recorded and used to create profiles of seismic velocities. The velocity profiles are interpreted to identify subsurface structures and material properties.

#### **7.5.2 Advantages**

- i. High Accuracy: Provides precise measurements of seismic velocities.

- ii. Detailed Subsurface Information: Useful for determining material properties and layer boundaries.
- iii. Effective for Site Characterization: Ideal for detailed investigations of specific sites.

### **7.5.3 *Disadvantages***

- i. Costly: Requires drilling and specialized equipment.
- ii. Limited Area of Investigation: Effective only for the area between the boreholes.
- iii. Complex Interpretation: Requires advanced data processing and interpretation skills.

### **7.5.4 *Application for Pipeline Maintenance***

CSP can be used to obtain detailed information about the subsurface conditions around pipelines. This is particularly useful for identifying areas of potential instability or changes in material properties that could affect the pipeline. After a catastrophic event, CSP can help assess the extent of damage and guide repair efforts.

## CHAPTER 8

# CONCLUSION

---

This thesis presents a comprehensive analysis of the seismic vulnerability and resilience of buried water pipelines in Guwahati City, Assam. The study evaluates the condition, vulnerabilities, and historical performance of the pipeline network, highlighting the critical need for improved earthquake resistance in the region. By applying the IITK-GSDMA guidelines, the research provides a robust framework for assessing and designing buried pipelines to withstand seismic events.

The development of an Excel sheet based on these guidelines, incorporating site-specific data for Guwahati derived from previous earthquake data and literature, offers a practical tool for engineers and planners. This tool facilitates the evaluation of pipeline performance under various seismic scenarios, ensuring a standards-aligned approach to enhance pipeline resilience.

Parametric studies conducted in this research reveal that increasing the pipe thickness significantly reduces the total axial strain experienced by pipelines under seismic loading conditions. This trend is consistent across all pipe diameters considered in the study (0.2 m, 0.4 m, 0.6 m, and 0.8 m), underscoring the importance of optimizing pipe thickness to mitigate seismic-induced strains.

The study also proposes the use of geophysical methods such as Electrical Resistivity Tomography (ERT) and Ground Penetrating Radar (GPR) for monitoring the functioning of pipelines after installation and following seismic events. These methods provide valuable site-specific data on soil properties and subsurface conditions, enhancing the accuracy of seismic risk assessments and informing maintenance and repair strategies.

In conclusion, this study contributes significantly to disaster risk reduction efforts in earthquake-prone regions like Assam. The holistic approach adopted in this research ensures the safety and reliability of vital buried infrastructure, providing a practical and effective strategy for enhancing the seismic resilience of buried pipelines.

## REFERENCES

---

1. Bandyopadhyay, S., Parulekar, Y. M., & Sengupta, A. (2022). Probabilistic seismic hazard assessment (PSHA) for the Assam region, incorporating site-specific amplification studies. *Environmental Earth Sciences*.
2. Baro, O., & Kumar, A. (2021). A review on the seismic vulnerability of oil and gas pipelines in Guwahati City.
3. Bartlett, S. F., & Youd, T. L. (1995). Empirical prediction of liquefaction-induced lateral spread. *Journal of Geotechnical Engineering*, 121(4), 316-329.
4. Bhadran, A., Duarah, B. P., Girishbai, D., Achu, A. L., Lahon, S., Jesiya, N. P., Vijesh, V. K., & Gopinath, G. (2024). Multi-model seismic susceptibility assessment for the 1950 Great Assam earthquake. *Geotechnical and Geological Engineering*.
5. Borah, M., Sharma, M. L., & Dubey, R. (2024). Comprehensive seismic hazard assessment for Assam, incorporating site-specific studies and a probabilistic approach. *Environmental Earth Sciences*.
6. Butchibabu, B., Khan, P. K., & Jha, P. C. (2021). Geophysical investigations for stability and safety mitigation of regional crude-oil pipeline near abandoned coal mines. *Journal of Geophysics and Engineering*, 18(1), 145-162.
7. Chenna, R., Terala, S., Singh, A. P., Mohan, K., Rastogi, B. K., & Ramancharla, P. K. (2014). Vulnerability assessment of buried pipelines: A case study. *Journal of Pipeline Systems Engineering and Practice*, 5(2), 04014003.
8. Dash, S. R., Sehgal, S., & Nair, G. (2015). Seismic vulnerability of pipelines in India. *Journal of Pipeline Systems Engineering and Practice*, 6(3), 04015001.
9. Gawande, K., Kiran, R., & Cherukuri, H. P. (2019). A numerical study of the response of buried steel pipelines undergoing strike-slip fault. *Journal of Pipeline Systems Engineering and Practice*, 10(4), 04019018.
10. Haque, C. H., & Choudhury, D. (2019). A comprehensive review of the seismic behavior of buried pipelines. *Geotechnical and Geological Engineering*, 37(5), 3981-4000.
11. Hongjing, L., Liu, J., & Baohua, Y. (2008) Response analysis of buried pipelines due to large ground movements. *Journal of Pipeline Systems Engineering and Practice*, 8(3), 04018012.
12. Inocente, I., Diaz, M., Gallardo, J., Maruyama, Y., Quiroz, L., & Zavala, C. (2023). Earthquake damage assessment of buried pipeline networks in the Lima Metropolitan Area (LMA), Peru. *Journal of Geophysics and Engineering*, 20(1), 145-162.

13. IITK-GSDMA Guidelines (2007). Guidelines for Seismic Design of Buried Pipelines. Indian Institute of Technology Kanpur and Gujarat State Disaster Management Authority.
14. Kaiser, A. E., Green, A. G., Campbell, F. M., Horstmeyer, H., Manukyan, E., Langridge, R. M., McClymont, A. F., Mancktelow, N., Finnemore, M., & Nobes, D. C. (2009) High-resolution seismic reflection imaging of the Alpine Fault, New Zealand. *Journal of Geophysical Research*, 114\*(B11), B11306.
15. Kanth, S. T. G., & Dash, S. K. (2008). Evaluation of seismic soil-liquefaction at Guwahati city. *Environmental Earth Sciences*, 61 (2), 355-368.
16. Lanzano, G., Salzano, E., Santucci de Magistris, F., & Fabbrocino, G. (2013). Performance assessment of continuous buried pipelines under earthquake loadings. *Journal of Pipeline Systems Engineering and Practice*, 4(2), 04013002.
17. Mandal, H. S., Shukla, A. K., Ghatak, M., Ranjan, R., & Mishra, O. P. (2011). Seismic intensity scenario in Guwahati City, Assam. *Natural Hazards*, 59(3), 1281-1298.
18. McClymont, A., Ernst, E., Bauman, P., & Payne, N. (2016). Integrating geophysical and geotechnical engineering methods for assessment of pipeline geohazards. *Proceedings of the International Pipeline Conference & Exposition IPC2016*, Calgary, Alberta, Canada.
19. Mukherjee, P., Khan, N. U., Prasad, B. B., & Nath, R. R. (2013). Seismic performance of buried continuous pipeline systems in Dehradun City, Uttarakhand, India. *Journal of Pipeline Systems Engineering and Practice*, 3(4), 04013001.
20. O'Rourke, M. J., & Liu, X. (1999). Response of Buried Pipelines Subject to Earthquake Effects. Multidisciplinary Center for Earthquake Engineering Research.
21. Raghavendra, K., & Baro, O. (2022). Liquefaction-induced lateral spreading potential of Guwahati city soil. *Journal of Geotechnical and Geoenvironmental Engineering*, 148(3), 04022012.
22. Solberg, I.-L., Hansen, L., Rønning, J. S., Haugen, E. D., Dalsegg, E., & Tønnesen, J. F. (2011). Combined geophysical and geotechnical approach to ground investigations and hazard zonation of a quick clay area, mid Norway. *Bulletin of Engineering Geology and the Environment*, 71(1), 119-133.
23. Wells, D. L., & Coppersmith, K. J. (1994). New empirical relationships among magnitude, rupture length, rupture width, rupture area, and surface displacement. *Bulletin of the Seismological Society of America*, 84(4), 974-1002.